

DOI: 10.1002/chem.201203867

# Regioselective Synthesis and Photophysical and Electrochemical Studies of 20-Substituted Cyanine Dye–Purpurinimide Conjugates: Incorporation of Ni<sup>II</sup> into the Conjugate Enhances its Tumor-Uptake and Fluorescence-Imaging Ability

Manivannan Ethirajan,<sup>[a]</sup> Ping Chen,<sup>[b]</sup> Tymish Y. Ohulchanskyy,<sup>[c]</sup> Lalit N. Goswami,<sup>[a]</sup> Anurag Gupta,<sup>[a]</sup> Avinash Srivatsan,<sup>[a]</sup> Mahabeer P. Dobhal,<sup>[a]</sup> Joseph R. Missert,<sup>[a]</sup> Paras N. Prasad,<sup>[c]</sup> Karl M. Kadish,<sup>\*,[b]</sup> and Ravindra K. Pandey<sup>\*,[a]</sup>

**Abstract:** We report herein a simple and efficient approach to the synthesis of a variety of *meso*-substituted purpurinimides. The reaction of *meso*-substituted purpurinimide with *N*-bromosuccinimide regioselectively introduced a bromo functionality at the 20-position, which on further reaction with a variety of boronic acids under Suzuki reaction conditions yielded the corresponding *meso*-substituted analogues. Interestingly, the free base and the metalated analogues showed remarkable differences in photosensitizing efficacy (PDT) and tumor-imaging ability. For example, the free-base conjugate showed significant *in vitro* PDT efficacy, but limited tumor avidity in mice bearing tumors, whereas the corresponding Ni<sup>II</sup> derivative did not produce any cell kill, but showed excellent tumor-imaging ability at a dose of

0.3  $\mu\text{mol kg}^{-1}$  at 24, 48, and 72 h post-injection. The limited PDT efficacy of the Ni<sup>II</sup> analogue could be due to its inability to produce singlet oxygen, a key cytotoxic agent required for cell kill in PDT. Based on electrochemical and spectroelectrochemical data in DMSO, the first one-electron oxidation (0.52 V vs. SCE) and the first one-electron reduction (−0.57–0.67 V vs. SCE) of both the free base and the corresponding Ni<sup>II</sup> conjugates are centered on the cyanine dye, whereas the second one-electron reduction (−0.81 V vs. SCE) of the two conjugates is assigned to the purpurinimide part of the molecule.

**Keywords:** C–C coupling · fluorescence · photodynamic therapy · photosensitizers · structure–activity relationships · tumor imaging

Reduction of the cyanine dye unit is facile and occurs prior to reduction of the purpurinimide group, which suggests that the cyanine dye unit as an oxidant could be the driving force for quenching of the excited triplet state of the molecules. An interaction between the cyanine dye and the purpurinimide group is clearly observed in the free-base conjugate, which compares with a negligible interaction between the two functional groups in the Ni<sup>II</sup> conjugate. As a result, the larger HOMO–LUMO gap of the free-base conjugate and the corresponding smaller quenching constant is a reason to decrease the intramolecular quenching process and increase the production of singlet oxygen to some degree.

## Introduction

Nontoxic porphyrin-based compounds in combination with harmless visible light, known as photodynamic therapy (PDT), have shown great potential in several biological applications, including cancer therapy and noncancerous treatments such as age-related macular degeneration (AMD) and cardiovascular and infectious diseases.<sup>[1–6]</sup> Since the approval of Photofrin<sup>®</sup>, a hematoporphyrin derivative (developed at the PDT Center, Roswell Park Cancer Institute, Buffalo, NY), our laboratories have been investigating the utility of naturally occurring chlorophyll and bacteriochlorophyll analogues for phototherapy and tumor imaging.<sup>[7]</sup> Among the chlorophyll-based analogues, HPPH [3-(1'-hexyloxyethyl)-3-devinylpyropheophorbide-*a*], which has a long-wavelength absorption at 665 nm (*in vivo*), has shown excellent photosensitizing efficacy in mice with limited skin phototoxicity, this being the main drawback with most other

[a] Dr. M. Ethirajan, Dr. L. N. Goswami, Dr. A. Gupta, Dr. A. Srivatsan, Dr. M. P. Dobhal, J. R. Missert, Prof. R. K. Pandey  
Chemistry Division, PDT Center, Cell Stress Biology  
Roswell Park Cancer Institute, Buffalo, NY, 14263 (USA)  
E-mail: ravindra.pandey@roswellpark.org

[b] Dr. P. Chen, Prof. K. M. Kadish  
Department of Chemistry, University of Houston  
Houston, TX, 77204-5003 (USA)  
E-mail: kkdish@uh.edu

[c] Dr. T. Y. Ohulchanskyy, Prof. P. N. Prasad  
Institute of Photonics and Biophotonics  
University of Buffalo (SUNY)  
Buffalo, NY 14221 (USA)

Supporting information for this article is available on the WWW under <http://dx.doi.org/10.1002/chem.201203867>.

porphyrin-based compounds.<sup>[8,9]</sup> HPPH is currently in Phase II human clinical trials for lung, esophagus, Barrett's esophagus, and head and neck cancers.<sup>[10–15]</sup> In our attempts to synthesize longer-wavelength photosensitizers (> 700 nm), we observed that replacing the five-membered isocyclic ring (e.g., HPPH,  $\lambda_{\text{max}}=660$  nm) with a six-membered fused imide ring system leads to a significant redshift (40–45 nm) in the electronic absorption spectra.<sup>[16]</sup> To investigate the effect of substituents on PDT efficacy, we have introduced the desired substituents at different positions of the purpurinimide system<sup>[17–19]</sup> (but not at the 20-position), as indicated in Figure 1. An *in vivo* biological investigation indicated

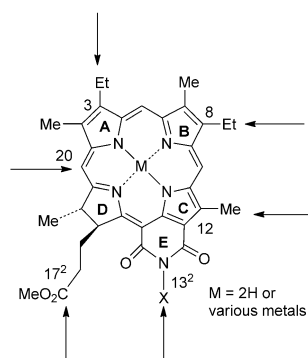


Figure 1. Various peripheral positions suitable for introducing the desired substituents into the purpurinimide system for structure–activity relationship studies.

that aside from the overall lipophilicity, the position of the substituents in the tetrapyrrolic skeleton also plays a crucial role in the long-term PDT response.<sup>[1,5]</sup>

Studies are underway in our laboratory (and others) to improve the target specificity of the PDT agents by conjugating the effective candidates with peptide and non-peptide-based compounds known to bind to receptors that are over-expressed in certain tumors.<sup>[20–22]</sup> Photosensitizers with high tumor avidity are also being used as vehicles to deliver the desired imaging agents (radionuclides for nuclear imaging, fluorophores for optical-imaging agents, Gd<sup>III</sup> chelates for MR imaging) to the target site.<sup>[22–26]</sup> This approach has shown great potential for the development of bifunctional agent(s) for the “see and treat” approach. Insertion of a metal, for example, nickel, into the photosensitizer–cyanine dye conjugate should eliminate its singlet oxygen yield and the metalated analogue may be useful as a fluorescence-imaging agent without any PDT capability. In recent years, PDT has also been evaluated for non-oncological applications, in particular, cationic photosensitizers have shown great promise for treating infectious diseases (bacterial, fungal, parasitic, and viral infections).<sup>[27,28]</sup> The rapid killing of bacteria by PDT and the unlikelihood of bacteria developing resistance to PDT suggests that this approach to treatment should be at the forefront of new therapies for infectious diseases.<sup>[29]</sup>

For quite some time, our laboratory has also been interested in developing an efficient method for the regioselective synthesis of 20-*meso*-substituted purpurinimides, which could be utilized for developing a variety of photosensitizers (cationic, anionic, and targeted analogues) and bifunctional agents (Figure 2).<sup>[30]</sup> This report shows the utility of the

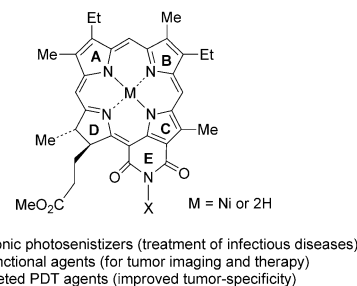


Figure 2. Modification of the purpurinimide skeleton.

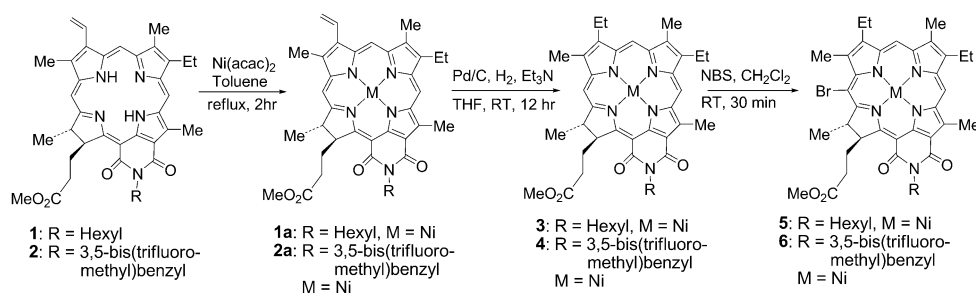
Suzuki reaction<sup>[31]</sup> in synthesizing such candidates by introducing an additional functionality into the photosensitizer and their application in developing efficient agents for fluorescence imaging with and without PDT. The regioselective introduction of a variety of substituents at the 20-*meso*-position by the Suzuki reaction also provides an opportunity to alter the overall lipophilicity and target specificity of the molecule(s) by varying the nature of the substitution.<sup>[31,32]</sup> If required, water-soluble analogues can be prepared by replacing the methyl ester functionality present at the 17<sup>2</sup>-position with appropriate hydrophilic functionalities.

## Results and Discussion

Among the growing number of palladium-catalyzed C–C coupling reactions, the Suzuki–Miyaura reaction<sup>[33,34]</sup> plays a leading role. The major advantages of this reaction are 1) the stability of the boron reagents, 2) the easy access to a broad variety of boronic acids, and 3) the tolerance for different functional groups. As a result of the simple experimental conditions, this reaction has been widely used for the preparation of a variety of biologically active molecules, including various porphyrin-based analogues. We herein present the utility of this synthetic approach in developing a variety of purpurinimides as possible target-specific photosensitizers and bifunctional agents for tumor imaging with and without PDT.

In this study, *N*-hexylpurpurinimide (**1**) and the corresponding *N*-[3,5-bis(trifluoromethyl)benzyl] analogue **2** were used as starting substrates. The Ni<sup>II</sup> complexes were obtained by treating these moieties with [Ni(acac)<sub>2</sub>] (acac = acetylacetonate) in toluene at reflux. Subsequent treatment of the intermediates with Pd/C under hydrogen afforded the Ni<sup>II</sup> mesopurpurinimides **3** and **4**, respectively (Scheme 1).

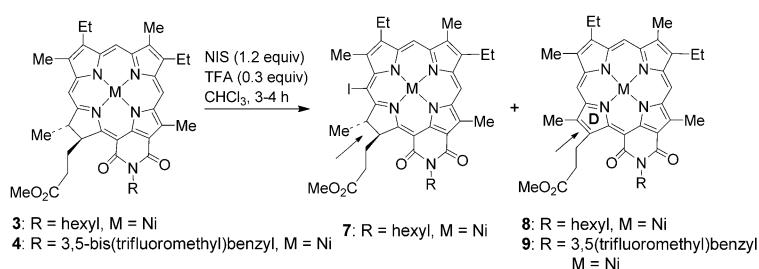
These metalated analogues, on stirring with *N*-bromosuccinimide (NBS) at room temperature for 30 min, produced



Scheme 1. Regioselective bromination of purpurinimides.

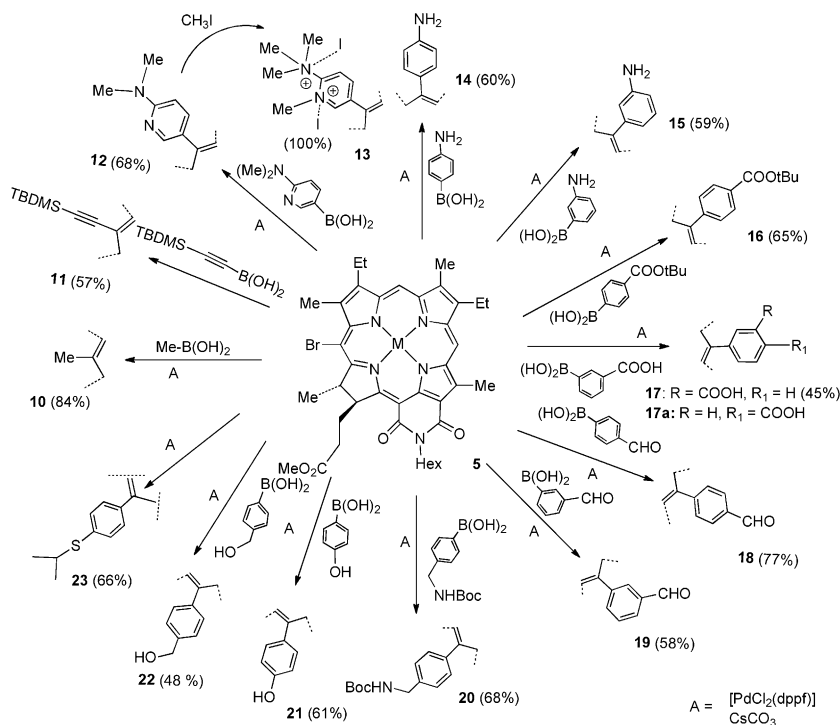
the corresponding Ni<sup>II</sup> 20-bromo-*N*-substituted-purpurinimides **5** and **6** in yields of 80 and 73 %, respectively.

To prepare 20-iodopurpurinimide, compound **3** was initially treated with *N*-iodosuccinimide (NIS) and, as expected, the desired iodo derivative **7** was isolated in a modest yield with the deiodinated analogue **8** being isolated in minor amounts (Scheme 2). However, subjecting the Ni<sup>II</sup> *N*-[3,5-bis-(trifluoromethyl)benzyl]meso-purpurinimide methyl ester **4** to similar conditions did not produce the desired 20-*meso*-iodo derivative, instead the purpurinimide **9** with the oxidized D ring was obtained as the major product.



Scheme 2. Effect of *N*-substitution in the iodination with NIS.

To further investigate the utility of the Suzuki reaction, Ni<sup>II</sup> 20-bromomesopurpurinimide **5** was treated with a series of functionalized boronic acids containing amino, formyl, carboxylic acid, or hydroxymethyl functionalities (Scheme 3). This approach was further extended by introducing *N,N*-dimethylaminopyridine and a furan group at the 20-position. Thus, *meso*-substituted analogues **10**–**22** were synthesized, all in good yield, except for the Ni<sup>II</sup> 20-(*p*-carboxyphenyl)-*N*-hexylpurpurinimide methyl ester **17a**. This compound was obtained in a yield of only 5 %, whereas the corresponding *m*-carboxy derivative **17** was isolated in a yield of 45 % under similar reaction conditions. This is the first report of the regioselective synthesis of 20-substituted purpurinimides, which provide an additional functionality for the preparation of biologically active compounds with the desired overall lipophilicity.



Scheme 3. Regioselective synthesis of 20-substituted purpurinimides by Suzuki reaction. The purpurinimide system allows the conjugation of these compounds to a series of DNA-intercalating and tumor-targeting moieties. Boc = *tert*-butoxycarbonyl, dppf = 1,1'-bis(diphenylphosphino)ferrocene, TBDMS = *tert*-butyldimethylsilyl.

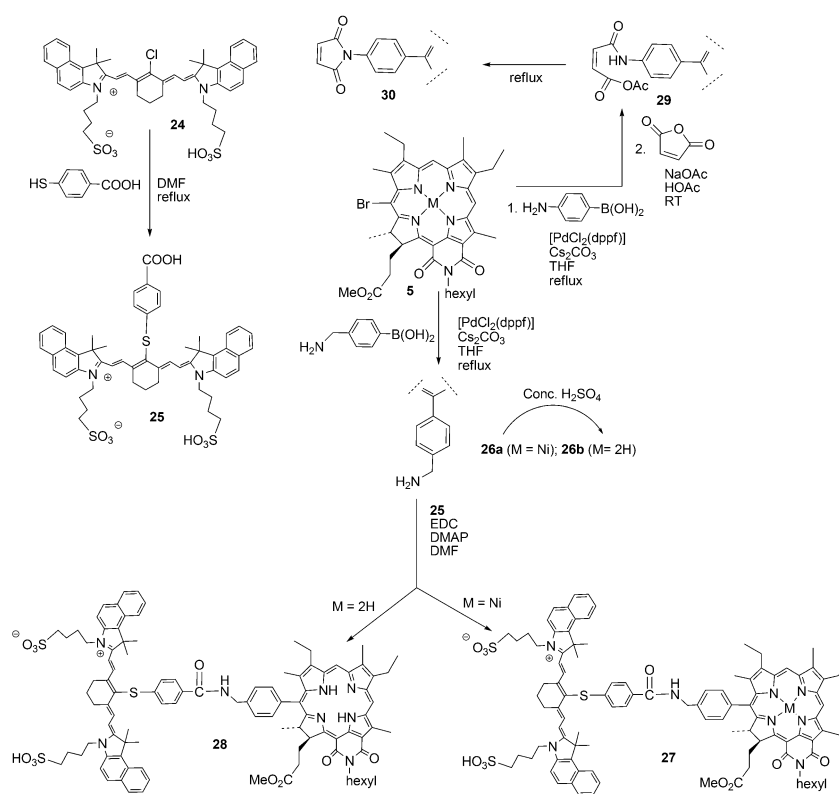
In recent years, the increasing occurrence of multi-antibiotic-resistant microbes has led to the search for alternative methods of killing pathogens and treating infections. PDT could be an alternate treatment for such infections. However, there are certain limitations because the delivery of visible light is, almost, by definition, a localized process. Therefore, PDT for infections is likely to be applied exclusively to localized disease as opposed to systemic infections. Phototherapy has also been used to treat animal models for dental infections.<sup>[35]</sup> In the first study, *Porphyromonas gingivalis*, one of the major causative organisms of periodontitis, was subjected to PDT on the buccal mucosa of the maxillary molars of rats with no visible bacteria.<sup>[36]</sup> Certain cationic photosensitizers have shown great promise in *Mycobacterium tuberculosis*, bacterial infections of *Candida albicans*, and parasite and viral infections.<sup>[37]</sup> In collaboration with the University of Rochester, certain cationic pyropheophorbide analogues, synthesized at Roswell Park, were evaluated for antimicrobial activity and a structure–activity relationship (SAR) study revealed that the number of cationic groups and their position in the molecule has a significant impact upon microbial inactivation.<sup>[38]</sup> The Suzuki approach presented in this paper allows the facile incorporation of a variable number of cationic groups into the purpurinimide system by following the approach used for the synthesis of compound **13**.

In an attempt to prepare a “bifunctional agent” for tumor imaging and phototherapy, we have previously shown that conjugates of tumor-avid photosensitizers (e.g., HPPH) and NIR-absorbing cyanine dyes can be used for tumor imaging and PDT.<sup>[1]</sup> Most conjugates synthesized to date consist of a flexible linker joining the two chromophores, which leads to possible folding within the molecule thus resulting in significant singlet oxygen quenching (a key cytotoxic agent for PDT). When folding occurs, the molecules are brought closer to each other, which could amplify the phenomenon known as Förster resonance energy transfer (FRET). The mechanism for FRET involves nonradiative energy transfer between two chromophores. For FRET to occur there needs to be spectral overlap between the fluorescence of the higher-energy chromophore and the absorbance of the lower-energy chromophore. These photosensitizer–cyanine dye conjugates exhibit such an overlap and there-

fore a portion of the imparted energy may transfer from the photosensitizer to the cyanine dye, thus decreasing the photosensitizer’s quantum yield of singlet oxygen.<sup>[39]</sup>

To develop an agent with decreased energy transfer and an improved quantum yield of singlet oxygen, one of our strategies was to combine the two moieties with a more rigid linker, as shown in Scheme 4. We were then able to prepare the desired purpurinimide–cyanine dye conjugates **27** and **28** by the Suzuki reaction. In brief, cyanine dye **25** was prepared by treating the commercially available **24** (IR-820) with 4-mercaptopropionic acid. The cyanine dye **25** was treated with Ni<sup>II</sup> 20-(*p*-aminomethylphenyl)purpurinImide **26a** to produce the purpurinimide–cyanine dye conjugate **27** in a yield of 35%. Similarly, the free base 20-(*p*-aminomethylphenyl)purpurinimide **26b** afforded the corresponding free-base analogue **28**. We have previously shown the utility of <sup>124</sup>I-pyropheophorbide-*a* analogues for positron emission tomography (PET)/fluorescence imaging.<sup>[22]</sup> To develop longer-wavelength purpurinimide-based “bifunctional agents”, maleimide analogue **30** can be converted into the corresponding free-base analogue **28**. We have previously shown the utility of <sup>124</sup>I analogue by following the methodology developed for the pyropheophorbide system.<sup>[40]</sup>

To investigate the utility of 20-(*p*-aminophenyl)mesopurpurinimide **14** in preparing a target-specific molecule, we were interested in introducing the maleimide moiety at the 20-position, which can be readily linked to various peptides and other tumor-targeting groups known for their target specificity towards receptors over-expressed in certain



Scheme 4. Simple approach for the preparation of tumor-targeting and bifunctional agents for tumor imaging. EDC=1-ethyl-3-(3-dimethylaminopropyl)carbodiimide).

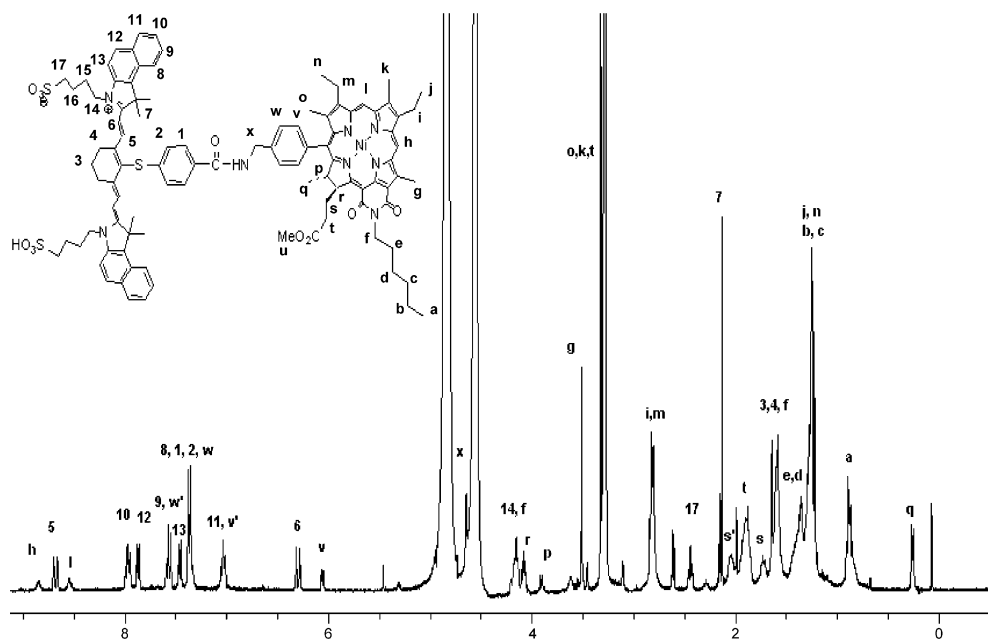


Figure 3.  $^1\text{H}$  NMR spectrum of the bifunctional agent **27** in a mixture of  $\text{CD}_3\text{OD}$  and  $[\text{D}_6]\text{DMSO}$ .

tumors.<sup>[41,42]</sup> To achieve our goal, bromopurpurinimide **5** was treated with maleic anhydride at room temperature. The intermediate **29** thus obtained was not isolated but heated at reflux with sodium acetate and acetic anhydride to give the maleimide **30** in an overall yield of 48%. This approach is quite versatile and provides an easy access to a variety of desired target molecules, including certain linear or cyclic peptides and monoclonal antibodies as well as a variety of target-specific photosensitizers.

The structure of each compound was confirmed by NMR, UV/Vis, and HRMS analyses and their purity ascertained by HPLC. As a representative example, the NMR spectrum of the photosensitizer–cyanine dye conjugate **27** is shown in Figure 3. The resonances of all the protons were confirmed by 2D NMR techniques (see the Supporting Information).

The absorption spectra for **26a** and **26b** are shown in Figure 4A, and those of the purpurinimide–cyanine dye conjugates **27** and **28**, along with that of **25**, are shown in Figure 4B. In comparison with the nonmetalated purpurinimide, the

longer-wavelength absorption of the corresponding metalated analogue shows a blueshift (Figure 4A). This behavior can also be observed in the absorption spectra of the pur-

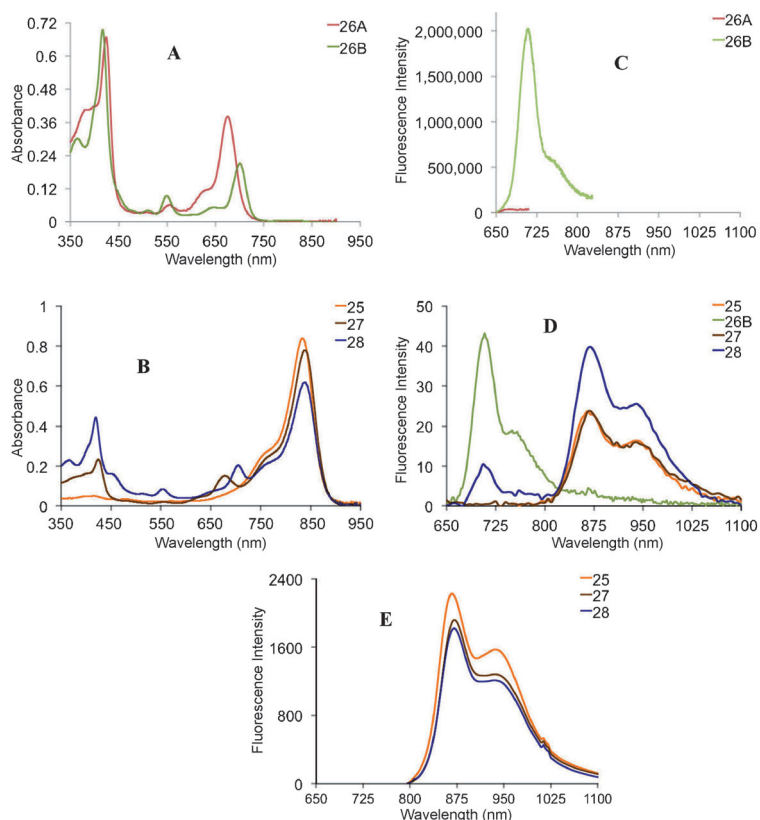


Figure 4. Absorption spectra of A) **26a** and **26b** and B) **25**, **27**, and **28**, and the fluorescence emission spectra for C) **26a** and **26b** when excited at 620 nm, D) **25**, **27**, and **28** when excited at 630 nm, and E) **25**, **27**, and **28** when excited at 785 nm. The concentration of all compounds was  $4 \mu\text{M}$  in methanol.

purinimide–cyanine dye conjugates **27** and **28** (Figure 4B). The long-wavelength absorption bands for the free base and nickel(II) purpurinimides are observed at 705 and 677 nm, respectively, and the cyanine dye moiety in both conjugates has an intense absorption peak at around 830 nm. The fluorescence characteristics of **27** and **28** are quite different. The fluorescence emission spectra displayed in Figure 4C and D show that in **26a** and **28**, the fluorescence emission of the photosensitizer (PS) moiety is quenched, which is associated with the presence of nickel(II).

In various bifunctional agents designed for fluorescence imaging and PDT, the existence of FRET between the PS and NIR fluorophores results in a decrease in the availability of singlet oxygen, which is directly correlated to PDT efficacy. To evaluate FRET in the conjugates, their fluorescence emissions were compared with those of the unconjugated PS. When **28** was excited at 630 nm, the fluorescence emission intensity of the cyanine dye increased by a factor of 1.7 compared with those of **25** and **27**, whereas the fluorescence emission intensity of the PS showed an approximate four-fold decrease compared with **26b** (Figure 4D). This suggests that energy is transferred from the PS to the cyanine dye. To prove that the cyanine dye portion of the conjugates could function independently of the PS, the conjugates were excited at 785 nm. The fluorescence emission intensity of **25** is higher than those of **27** and **28** by around 300 a.u. However, the difference in the fluorescence intensities of **27** and **28** is less than 70 a.u.. These results suggest that the cyanine dye in the conjugate can indeed function independently of the PS when excited at 785 nm.

**Singlet oxygen production for 25, 26a, 26b, 27, 28, and HPPH:** The production of singlet oxygen is one of the requirements for effective PDT. The singlet oxygen producing efficiencies of compounds **25**, **26a**, **26b**, **27b**, **28**, and HPPH were evaluated by measuring the phosphorescence of singlet oxygen at 1270 nm upon excitation at 532 nm (Figure 5).

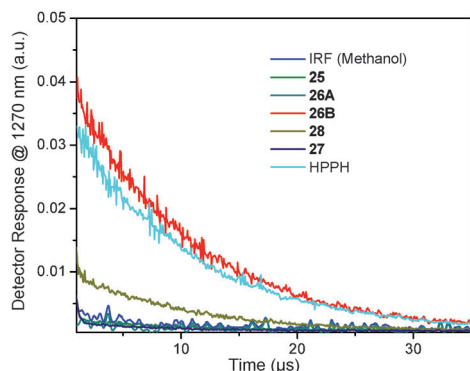


Figure 5. Singlet oxygen production of **25**, **26a**, **26b**, **27**, **28**, and HPPH in methanol detected by measuring the phosphorescence of singlet oxygen at 1270 nm upon excitation with a 532 nm laser. The instrument response function (IRF) of methanol is also shown. The singlet oxygen production of HPPH is shown as a reference ( $\Phi_{\Delta} = 48\%$  for HPPH in methanol).

The singlet oxygen decay curve of methanol was used as a measure of the instrument response function (IRF) and HPPH was used as a reference because of its known singlet oxygen quantum yield ( $\Phi_{\Delta} = 48\%$ <sup>[8]</sup>). From the singlet oxygen decay curves (Figure 5) it can be seen that **26b** gives the highest singlet oxygen yield and that conjugate **27** shows limited singlet oxygen producing ability. Singlet oxygen luminescence studies also confirmed that the presence of Ni<sup>II</sup> as the central metal significantly diminishes the singlet oxygen producing ability of the photosensitizer.

**Photostability of 27 and 28:** To a certain extent, the photostability of the photosensitizer during light treatment is important for optimizing the PDT response. Therefore the photostability of **27** and **28** was measured in 17% bovine calf serum (BCS) by irradiating their solutions at 677 and 705 nm, respectively, with a light dose equivalent of 75 mW cm<sup>-2</sup> at the center plane of the cuvette. The absorbance intensity of the cyanine dye portion of the conjugates **27** and **28** was monitored at 852 and 849 nm, respectively, and the percent-normalized absorbance was recorded as a function of time. The photostability of **27** and **28** are shown in Figure 6C. Based on the singlet oxygen luminescence measurements, **27** should be more stable as negligible amounts of singlet oxygen will be generated by irradiating the metalated photosensitizer with light of an appropriate wavelength. As expected, the absorbance of the cyanine dye moiety of conjugate **28** had decreased to approximately 6% of its initial value 21 min post-irradiation, whereas the cyanine dye moiety of **27** (containing the free-base photosensitizer) had photobleached to 72% of the initial value 78 min post-irradiation. These data confirm that the presence of Ni<sup>II</sup> in the purpurinimide core enhances the photostability of the photosensitizer and reduces its singlet oxygen producing ability.

**Electrochemistry and spectroelectrochemistry:** The redox properties of the cyanine dye (**25**) and its purpurinimide nickel (**27**) and free-base (**28**) conjugates were examined in DMSO containing 0.1 M tetrabutylammonium perchlorate (TBAP) to determine whether the central metal ion in the purpurinimide of the conjugates influences the electron-accepting and -donating properties. Examples of the cyclic voltammograms of these three compounds are shown in Figure 7.

The cyanine dye **25** undergoes a reversible one-electron oxidation at  $E_{1/2} = 0.56$  V and a reversible one-electron reduction at  $E_{1/2} = -0.56$  V in DMSO containing 0.1 M TBAP with an additional irreversible reduction also seen at  $E_p = -1.40$  V at a scan rate of 0.1 V s<sup>-1</sup>. Under the same conditions, the two conjugates undergo an oxidation at similar potentials of  $E_{1/2} = 0.52$  V (**27**) and 0.53 V (**28**), two reversible reductions at  $E_{1/2} = -0.57$  and  $-0.81$  V (**27**) and  $-0.67$  and  $-0.81$  V (**28**), and an additional irreversible reduction at  $E_p = -1.36$  V (**27**) and  $-1.30$  V (**28**) at a scan rate of 0.1 V s<sup>-1</sup> (see Figure 7). A comparison of the potentials of the three compounds suggests that the first oxidation and

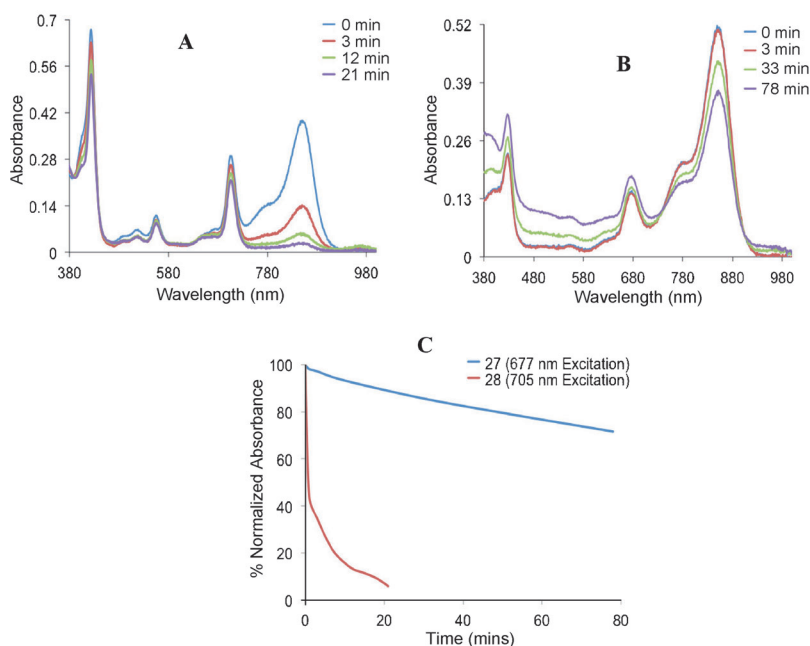


Figure 6. A) Absorption spectra of conjugate **28** in 17% BCS during the photobleaching process. B) Absorbance spectra for conjugate **27** in 17% BCS during the photobleaching process. C) Comparison of photobleaching rates for conjugates **27** and **28**. The solutions were irradiated at 677 (**27**) and 705 nm (**28**) with a laser power of 530 mW.

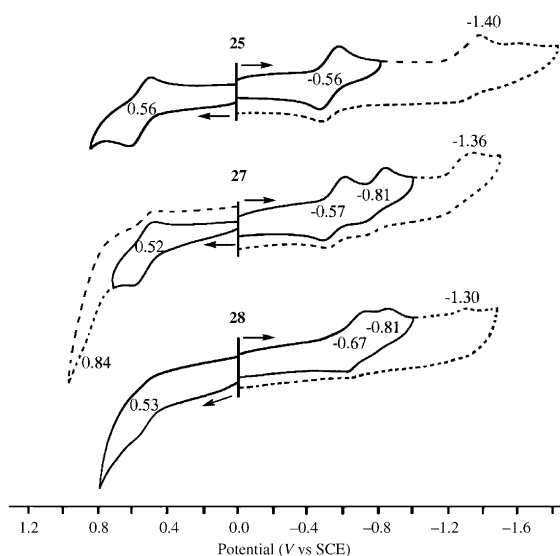


Figure 7. Cyclic voltammograms of **25**, **27**, and **28** in DMSO containing 0.1 M TBAP. Scan rate = 0.1 V s<sup>-1</sup>.

the first and third reductions of both **27** and **28** all involve the cyanine dye portion of the molecule and thus the second one-electron reduction of the two conjugates at  $E_{1/2} = -0.81$  V can confidently be assigned to the purpurinimide part of the molecule.

More definitive evidence for these assignments is given by the thin-layer spectroelectrochemical data presented in Figures 8 and 9. The spectrum of neutral **25** in DMSO contain-

ing 0.1 M TBAP is characterized by an intense, split near-IR band at 773 and 849 nm, whereas **27** and **28** in their neutral forms exhibit spectra that are a simple sum of the absorptions of the individual cyanine and purpurinimide units. For example, the 426 and 674 nm bands of **27** in DMSO can be attributed to the Ni<sup>II</sup> purpurinimide unit,<sup>[42]</sup> whereas the intense, split near-IR band at 773 and 850 nm of **27** has been attributed to contributions from the cyanine dye unit (see the top of Figure 8b). Applying a reduction potential of  $-0.70$  V to a solution of **27** in DMSO containing 0.1 M TBAP led to the disappearance of the split near-IR band at 773 and 850 nm and the appearance of a new visible band at 531 nm (Figure 8b). No change is observed in the Ni<sup>II</sup> purpurinimide bands of **27** (426 and 674 nm) during this one-

electron reduction whereas the cyanine dye bands undergo exactly the same spectral changes as seen during the reduction of **25** at  $-0.70$  V in the thin-layer cell (Figure 8a). This unambiguously indicates that the first one-electron addition to the conjugate **27** involves the cyanine portion of the molecule.

Shifting the applied potential from  $-0.70$  to  $-1.00$  V for a DMSO solution of **27** led to a decrease in the intensity of the 426 and 674 nm bands (Figure 8b), similar to the spectral changes reported in the literature<sup>[42]</sup> for the first reduction of Ni<sup>II</sup> purpurinimide, which suggests that the second electron is added to the Ni<sup>II</sup> purpurinimide part of the molecule. The third reduction of **27** at  $-1.50$  V is centered on the cyanine dye, based on the similar spectral changes observed during controlled reduction of **25** at  $-1.60$  V (Figure 8a).

The electron-transfer site of the oxidation can also be assigned on the basis of the data shown in Figure 9, which shows almost identical spectral changes for **25** and **27** under the same solution conditions, indicating that the first oxidation of **27** occurs in the cyanine portion of the molecule. The same initial sites for the redox processes are proposed for conjugate **28**, and the thin-layer spectral changes of **28** during each redox process for this compound are presented in Figure S1 in the Supporting Information.

Both the first oxidation and the first reduction of conjugates **27** and **28** are centered on the cyanine dyad with their first oxidation potential negatively shifted by 30–40 mV in comparison with that of **25** due to the influence of the linked purpurinimide functional agent. Almost identical half-wave potentials for the first reduction can be seen for

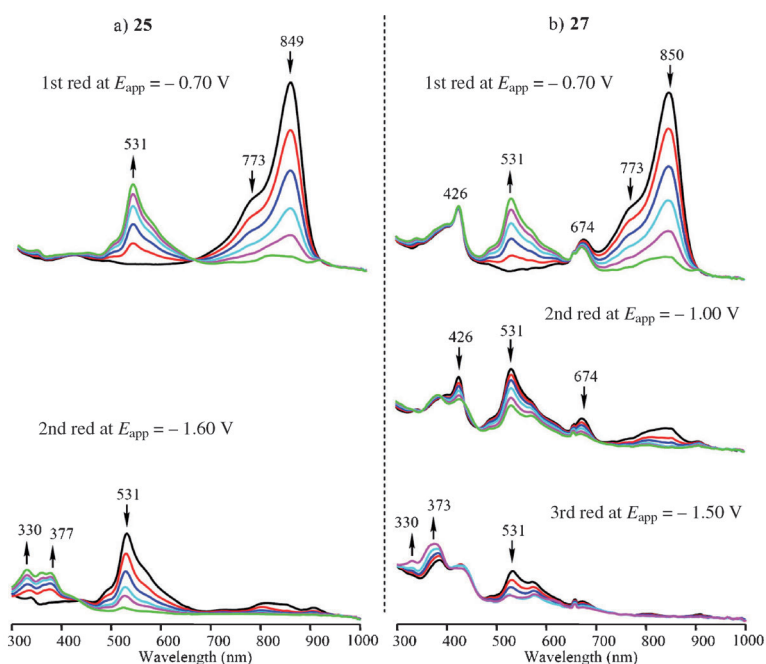


Figure 8. Thin-layer UV/Vis spectra of a) **25** and b) **27** during controlled reductions in DMSO containing 0.1 M TBAP.

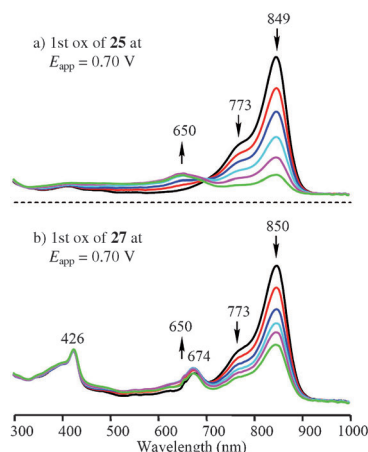


Figure 9. Thin-layer UV/Vis spectra of a) **25** and b) **27** during the first oxidation in DMSO containing 0.1 M TBAP.

cyanine dyad **25** and conjugate **27**, but a potential difference of 110 mV is seen for the first reduction of **28**. The fact that the cyanine dyad is reduced at a more negative potential suggests electron communication between the cyanine dye and the purpurinimide portion of the molecule. In other words, the two functional agents are fairly interactive with each other in the case of **28** whereas they are “almost independent” of each other in the case for **27**.

For the conjugates **27** and **28**, reduction of the cyanine dye unit is easier than reduction of the purpurinimide unit ( $E_{1/2} = -0.57$  to  $-0.67$  V vs. SCE,  $-0.3$  to  $-0.4$  V vs. SHE). Thus, the cyanine dye unit could be used as an oxidant to quench the excited triplet state of the purpurinimide

unit.<sup>[43,44]</sup> According to the Rehm–Weller equation,<sup>[45]</sup> the quenching constant would approximately depend on the potential difference between the first oxidation and the first reduction (the electrochemical HOMO–LUMO gap) for molecules with similar structures. The HOMO–LUMO gaps of 1.09 V (**27**) and 1.20 V (**28**) show that compound **28**, which has a larger HOMO–LUMO gap, will have a smaller electron-transfer driving force and avoid quenching of the excited triplet state. In the case of **28**, this makes it possible to produce more singlet oxygen by collision of an oxygen molecule with the excited triplet state. This is consistent with data for the phosphorescence of singlet oxygen for these compounds provided earlier.

#### Comparative in vitro photosensitizing efficacy of metalated versus nonmetalated analogues:

Conjugate **28** and the corresponding Ni<sup>II</sup> analogue **27** were evaluated for in vitro photosensitizing efficacy in the murine colon carcinoma (Colon-26) cell line by using the MTT-based phototoxicity assay.<sup>[46]</sup> In brief, cells were incubated with increasing concentrations of the photosensitizers for 24 h and then illuminated with light at 706 nm for conjugate **28** and at 680 nm for conjugate **27**. Neither compound exhibited dark (drug, no light) toxicity (cell death), even at higher doses (6  $\mu\text{M}$ ). As expected, the conjugate **27**, which contains a Ni<sup>II</sup> photosensitizer, showed limited singlet oxygen producing efficiency, and upon exposure to light it also showed minimal PDT efficacy in comparison with the nonmetalated derivative **28**. The results are summarized in Figure 10 and are represented in two ways: A) At a fixed drug concentration (1.0  $\mu\text{M}$ ) with variable light doses and B) at a fixed light dose with variable concentrations of the drugs. As can be seen, the free-base conjugate **28** showed significant PDT efficacy, whereas, under similar treatment conditions, the corresponding Ni<sup>II</sup> derivative **27** did not exhibit any cell kill, which could be due to its limited singlet oxygen producing ability.

#### Compound 27 with NiII as the central metal showed significantly improved tumor contrast by fluorescence imaging:

The fluorescence imaging potentials of conjugates **27** and **28** were investigated in mice bearing Colon-26 tumors. Both photosensitizers, at a dose of 0.3  $\mu\text{mol kg}^{-1}$ , were injected (intravenously) and the mice were imaged at 24 h post-injection. The results depicted in Figure 11 reveal that compared with the free base **28**, the corresponding Ni<sup>II</sup> complex **27**

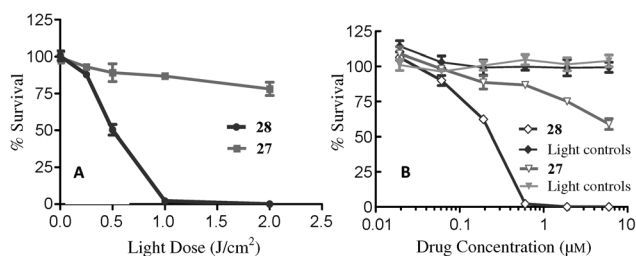


Figure 10. In vitro photosensitizing efficacy (MTT assay) of Ni<sup>II</sup> purpurinimide-cyanine dye conjugate **27** and the corresponding nonmetalated analogue **28**. A) PDT efficacy at a fixed concentration of the photosensitizers with the cells exposed to variable light doses. B) PDT efficacy at a fixed light dose and variable concentrations. On exposing the cells to light without incubation with photosensitizers **27** and **28**, no dark toxicity (cell kill) was observed. The cells were incubated for 24 h before exposure to light.

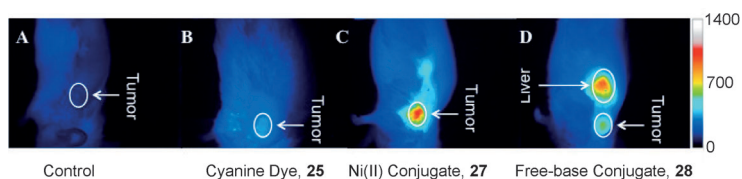


Figure 11. Whole-body fluorescence imaging of A) a control mouse, B) cyanine dye **25**, C) conjugate **27**, and D) conjugate **28** at a dose of 0.3 µmol/kg at 24 h post intravenous injection.

showed improved tumor uptake and specificity. The best tumor contrast was observed at 24 and 48 h post-injection (see the Supporting Information). On the other hand, the free-base analogue **28** showed a significantly higher uptake in other organs (liver, kidney, and spleen) than that seen in the tumor. Under similar imaging parameters, the cyanine dye **25** alone did not show any tumor-imaging ability (data not shown), which clearly indicates that conjugation of the non-tumor-specific cyanine dye, which possesses the required photophysical properties, with tumor-avid purpurinimide-based photosensitizers enhances its tumor specificity. This approach also provides a great platform for the development of imaging agents with and without PDT capability. To enhance the PDT capability of conjugate **28**, it is important to change the overall lipophilicity of the molecule, which should make a significant difference to its tumor uptake and pharmacokinetic and -dynamic characteristics. These studies are in progress.

## Conclusion

We have shown the utility of the Suzuki reaction for the synthesis of certain purpurinimide-based conjugates for tumor imaging and therapy. The synthetic approach discussed herein is not only limited to the purpurinimide system but can be extended to a wide variety of chlorin and bacteriochlorin systems. The ability to introduce additional functionality into a photosensitizer provides additional tools for introducing desired tumor-targeting moieties at a partic-

ular position and also to alter the overall lipophilicity at other position(s) of the molecule to gain the desired pharmacokinetics. A molecule with multiple functionalities could also help in developing “multifunctional” agents for imaging and therapy. Thus, a single agent could be used for imaging and therapy by following a “See and Treat” approach. This study also illustrates the presence of metal in the photosensitizer-cyanine dye conjugates has a significant effect not only on its photophysical properties, but also in tumor localization. Such properties may vary with the nature of the central metal in the porphyrin core and studies along this line are in progress. The higher in vivo uptake of the Ni<sup>II</sup> purpurinimide-cyanine dye conjugate compared with the corresponding free-base analogue reveals a remarkable difference in the biodistribution between the two conjugates.

The regioselective synthesis of 20-bromopurpurinimide (chlorin) and its further elaboration could also allow the facile development of a wide variety of supramolecular structures as models for photosynthetic reaction centers, semiconductors for use in hybrid electronics, optoelectronic applications, electrochemical sensors, and receptor models with unique photophysical and electrochemical properties.

The investigated functional agents are electrochemically active and systematic electrochemical and spectroelectrochemical studies on these photosensitizers with “multifunctional” agents have been carried out. Their redox potentials, electron-transfer sites, and UV/Vis spectra have been investigated in different oxidation states. Furthermore, analysis of the electrochemical data shows the stability of the conjugates and the interaction that occurs between the two functional agents in the donor-acceptor system. Detailed photophysical studies (fluorescence lifetime, quantum yield, comparative in vitro/in vivo photobleaching of the photosensitizer and the cyanine dye) are in progress and will be published separately.

## Experimental Section

All reactions were carried out in flame-dried glassware under an atmosphere of nitrogen with magnetic stirring. TLC was carried out on ANALTECH precoated silica gel GF PE sheets (Cat. 159017, layer thickness 0.25 mm) and aluminum oxide NF PE sheets (Cat. 101016, layer thickness 0.2 mm). Column chromatography was performed either on silica gel 60 (70–230 mesh) or neutral alumina (Brockmann grade III, 50 mesh). In some cases preparative TLC plates were also used for the purification (ANALTECH precoated silica gel GF glass plate, Cat. 02013, layer thickness 1.0 mm). Solvents were purified as follows: Trace amounts of water and oxygen from THF were removed by heating at reflux over sodium under an inert atmosphere and dichloromethane was dried over P<sub>2</sub>O<sub>5</sub>. Anhydrous DMF, triethylamine, pyridine, and other common chromatographic solvents were obtained from commercial suppliers (J.T. Baker, EMD, and Aldrich) and used without further purification. NMR spectra were recorded on a Bruker DRX 400 MHz spectrometer. All chemical shifts are reported in parts per million (δ). <sup>1</sup>H NMR (400 MHz) spectra were recorded at room temperature in CDCl<sub>3</sub> or CD<sub>3</sub>OD solutions and referenced to residual CHCl<sub>3</sub> (7.26 ppm) or TMS (0.00 ppm). EI-mass spectra were recorded on a Bruker Esquire ion-trap mass spectrometer equipped with a pneumatically assisted electrospray ionization source operating in positive mode. HRMS analyses were per-

formed at the Mass Spectrometry Facility, Michigan State University. UV/Vis spectra were recorded on a Varian Cary 50 Bio UV/Visible spectrophotometer using dichloromethane as solvent. All photophysical experiments were carried out by using spectroscopic-grade solvents. Most of the purpurinimides and the corresponding cyanine dye conjugates tend to decompose at  $>150^{\circ}\text{C}$ , which made it extremely difficult to measure a precise melting point.

**Ni<sup>II</sup> mesopurpurin-18-N-hexylimide methyl ester (3):** Ni<sup>II</sup> purpurin-18-N-hexylimide (**1a**; 350.0 mg, 0.48 mmol) was dissolved in distilled THF (100 mL). Pd/C (10% w/w, 350.0 mg) and 5–6 drops of triethylamine were added to the reaction mixture, which was degassed and flushed with H<sub>2</sub> and vigorously stirred for 12 h under H<sub>2</sub>. The progress of the reaction was monitored by UV/Vis and <sup>1</sup>H NMR spectroscopy. After completion of the reaction, the mixture was degassed, flushed with N<sub>2</sub>, and filtered over a bed of Celite. The filtrate was concentrated and the crude product purified through a column of silica by using 0.5–1% acetone/dichloromethane as eluent. Yield: 300.0 mg (85.4%). <sup>1</sup>H NMR (400 MHz, CDCl<sub>3</sub>):  $\delta$  = 8.99 (s, 1H; *meso*-H), 8.61 (s, 1H; *meso*-H), 7.86 (s, 1H; *meso*-H), 4.78 (dd,  $J$  = 3.2, 9.2 Hz, 1H; 17-H), 4.27 (m, 2H; N-CH<sub>2</sub>-Hexyl), 4.03 (q,  $J$  = 7.2 Hz, 1H; 18-H), 3.60 (s, 3H; CO<sub>2</sub>Me), 3.48 (s, 3H; ring-CH<sub>3</sub>), 3.44–3.36 (m, 4H; 3-CH<sub>2</sub>CH<sub>3</sub>, 8-CH<sub>2</sub>CH<sub>3</sub>), 2.95 (s, 3H; ring-CH<sub>3</sub>), 2.87 (s, 3H; ring-CH<sub>3</sub>), 2.64–2.54 (m, 2H; 17<sup>2</sup>-CH<sub>2</sub>), 2.20–2.18 (m, 1H; 17<sup>1</sup>-CHH), 1.94–1.92 (m, 1H; 17<sup>1</sup>-CHH), 1.87–1.82 (m, 2H; CH<sub>2</sub>-Hexyl), 1.55–1.48 (m, 8H; 3-CH<sub>2</sub>CH<sub>3</sub>, 8-CH<sub>2</sub>CH<sub>3</sub>, CH<sub>2</sub>-Hexyl), 1.44–1.36 (m, 4H; 2 CH<sub>2</sub>-Hexyl), 1.33 (d,  $J$  = 6.8 Hz, 3H; 18-CH<sub>3</sub>), 0.92 ppm (t,  $J$  = 7.2 Hz, 3H; CH<sub>3</sub>-Hexyl); <sup>13</sup>C NMR (100 MHz, CDCl<sub>3</sub>):  $\delta$  = 173.8, 166.8, 162.9, 162.3, 160.7, 150.4, 147.1, 144.8, 143.6, 141.5, 140.2, 138.3, 135.8, 133.3, 128.8, 128.4, 126.0, 119.6, 108.5, 102.3, 97.7, 94.5, 53.3, 51.5, 47.4, 41.9, 39.9, 32.0, 31.7, 28.8, 27.0, 22.7, 20.9, 19.1, 17.1, 16.8, 14.0, 12.2, 10.6 ppm; UV/Vis (CH<sub>2</sub>Cl<sub>2</sub>):  $\lambda_{\text{max}}$  ( $\epsilon$ ) = 661 nm ( $3.2 \times 10^4 \text{ M}^{-1} \text{ cm}^{-1}$ ); MS (EI):  $m/z$ : 721 [M+H]<sup>+</sup>; HRMS: calcd for C<sub>40</sub>H<sub>47</sub>N<sub>5</sub>NiO<sub>4</sub>: 719.2982; found: 719.2971.

**Ni<sup>II</sup> N-Bis(3,5-trifluoromethyl)benzylpurpurin-18-N-hexylimide methyl ester (2a):** N-Bis(3,5-trifluoromethyl)benzylpurpurin-18-N-hexylimide (**2**; 200.0 mg, 0.25 mmol) was dissolved in toluene (50 mL) and nickel acetylacetonate hydrate (640.0 mg, 2.45 mmol) was added. The reaction mixture was heated at reflux vigorously for 2 h and the progress of the reaction was monitored by TLC and UV/Vis spectrophotometry. After completion of the reaction, the mixture was cooled and directly loaded onto a column of silica. The product **2a** was eluted with 1% acetone/dichloromethane. Yield: 195.0 mg (91.1%). <sup>1</sup>H NMR (400 MHz, CDCl<sub>3</sub>):  $\delta$  = 9.00 (s, 1H; *meso*-H), 8.73 (s, 1H; *meso*-H), 8.09 (s, 2H; Ph-H), 7.91 (s, 1H; *meso*-H), 7.78 (s, 1H; Ph-H), 7.55 (dd,  $J$  = 11.6, 17.6 Hz, 1H; CH=CH<sub>2</sub>), 5.93 (d,  $J$  = 10.4 Hz, 1H; CH=CH<sub>2</sub>), 5.91 (d,  $J$  = 4.0 Hz, 1H; -CH=CH<sub>2</sub>), 5.59 (s, 2H; N-CH<sub>2</sub>-Ph), 4.72 (m, 1H; 17-H), 4.06 (q,  $J$  = 7.2 Hz, 1H; 18-H), 3.60 (s, 3H; CO<sub>2</sub>Me), 3.49 (s, 3H; ring-CH<sub>3</sub>), 3.40 (m, 2H; 8-CH<sub>2</sub>CH<sub>3</sub>), 2.98 (s, 3H; ring-CH<sub>3</sub>), 2.93 (s, 3H; ring-CH<sub>3</sub>), 2.63–2.56 (m, 2H; 17<sup>2</sup>-CH<sub>2</sub>), 2.19 (m, 1H; 17<sup>1</sup>-CH<sub>2</sub>), 1.92 (m, 1H; 17<sup>1</sup>-CH<sub>2</sub>), 1.50 (t,  $J$  = 7.2 Hz, 3H; 8-CH<sub>2</sub>CH<sub>3</sub>), 1.32 ppm (d,  $J$  = 6.8 Hz, 3H; 18-CH<sub>3</sub>); <sup>13</sup>C NMR (100 MHz, CDCl<sub>3</sub>):  $\delta$  = 173.6, 166.8, 162.9, 162.5, 160.5, 150.0, 145.6, 144.1, 143.8, 141.0, 140.0, 138.7, 135.6, 134.2, 134.0, 131.7, 131.3, 128.8, 128.5, 124.7, 121.1, 121.5, 119.1, 108.9, 104.4, 97.1, 95.1, 53.6, 51.5, 47.4, 42.1, 32.0, 29.6, 28.8, 20.8, 19.0, 17.0, 12.3, 11.6, 10.6 ppm; UV/Vis (CH<sub>2</sub>Cl<sub>2</sub>):  $\lambda_{\text{max}}$  ( $\epsilon$ ) = 675 nm ( $4.1 \times 10^4 \text{ M}^{-1} \text{ cm}^{-1}$ ); MS (EI):  $m/z$ : 861 [M+H]<sup>+</sup>; HRMS: calcd for C<sub>43</sub>H<sub>37</sub>F<sub>6</sub>N<sub>5</sub>NiO<sub>4</sub>: 859.2103; found: 859.2107.

**Ni<sup>II</sup> N-Bis(3,5-trifluoromethyl)benzylmesopurpurin-18-N-hexylimide methyl ester (4):** Purpurinimide **2a** (300.0 mg, 0.34 mmol) was dissolved in distilled THF (100 mL). Pd/C (10% w/w, 600.0 mg) and 5–6 drops of triethylamine were added to the reaction mixture, which was flushed with H<sub>2</sub> and stirred vigorously for 12 h under H<sub>2</sub>. The progress of the reaction was monitored by UV/Vis and <sup>1</sup>H NMR spectroscopy. After completion of the reaction, the mixture was degassed, flushed with N<sub>2</sub>, and filtered over a bed of Celite. The filtrate was concentrated and the crude product was purified through a column of alumina (G-III) by using 0.5–1% acetone/dichloromethane as eluent. Yield: 280.0 mg (93.1%). <sup>1</sup>H NMR (400 MHz, CDCl<sub>3</sub>):  $\delta$  = 8.98 (s, 1H; *meso*-H), 8.59 (s, 1H; *meso*-H), 8.08 (s, 2H; Ph-H), 7.85 (s, 1H; *meso*-H), 7.77 (s, 1H; Ph-H), 5.58 (s, 2H; N-CH<sub>2</sub>-Ph), 4.71 (dd,  $J$  = 3.60, 8.80 Hz, 1H; 17-H), 4.04 (q,  $J$  = 7.2 Hz, 1H;

18-H), 3.58 (s, 3H; CO<sub>2</sub>Me), 3.46 (s, 3H; ring-CH<sub>3</sub>), 3.42–3.34 (m, 4H; 3-CH<sub>2</sub>CH<sub>3</sub>, 8-CH<sub>2</sub>CH<sub>3</sub>), 2.94 (s, 3H; ring-CH<sub>3</sub>), 2.86 (s, 3H; ring-CH<sub>3</sub>), 2.62–2.55 (m, 2H; 17<sup>2</sup>-CH<sub>2</sub>), 2.16–2.13 (m, 1H; 17<sup>1</sup>-CH<sub>2</sub>), 1.93–1.89 (m, 1H; 17<sup>1</sup>-CH<sub>2</sub>), 1.55–1.48 (m, 6H; 3-CH<sub>2</sub>CH<sub>3</sub>, 8-CH<sub>2</sub>CH<sub>3</sub>), 1.32 ppm (d,  $J$  = 6.8 Hz, 3H; 18-CH<sub>3</sub>); <sup>13</sup>C NMR (100 MHz, CDCl<sub>3</sub>):  $\delta$  = 189.6, 173.7, 166.8, 162.9, 162.5, 161.1, 150.9, 147.4, 145.0, 143.9, 141.1, 140.6, 138.4, 137.5, 135.2, 134.5, 134.1, 133.5, 133.1, 131.8, 131.3, 128.8, 118.7, 108.9, 102.5, 97.1, 94.8, 53.4, 51.5, 47.4, 42.1, 32.0, 29.6, 28.8, 20.8, 19.0, 17.0, 16.7, 12.3, 10.6 ppm; UV/Vis (CH<sub>2</sub>Cl<sub>2</sub>):  $\lambda_{\text{max}}$  ( $\epsilon$ ) = 664 nm ( $3.2 \times 10^4 \text{ M}^{-1} \text{ cm}^{-1}$ ); MS (EI):  $m/z$ : 863 [M+H]<sup>+</sup>; HRMS: calcd for C<sub>43</sub>H<sub>39</sub>F<sub>6</sub>N<sub>5</sub>NiO<sub>4</sub>: 861.2260; found: 861.2263.

**Ni<sup>II</sup> 20-Bromomesopurpurin-N-hexylimide methyl ester (5):** In a 100 mL dry round-bottomed flask, Ni mesopurpurin-N-hexylimide (**3**; 50.0 mg, 0.069 mmol) was dissolved in dry CH<sub>2</sub>Cl<sub>2</sub> (30.0 mL). N-Bromosuccinimide (14.8 mg, 0.083 mmol) was added to this solution and the resultant mixture was stirred for 30 min at room temperature under N<sub>2</sub>. The progress of the reaction was monitored by UV/Vis spectrophotometry and TLC. After completion of the reaction, saturated sodium bicarbonate (50.0 mL) was gradually added to the reaction mixture and then extracted with dichloromethane (3 × 50.0 mL). The organic layers were collected, combined, and washed with water (100.0 mL). The organic layer was separated, dried over anhydrous Na<sub>2</sub>SO<sub>4</sub>, and the solvent was evaporated. The crude product obtained was purified through a column of silica by using 1–2% acetone/dichloromethane as eluent. Yield: 45.0 mg (81.2%) <sup>1</sup>H NMR (400 MHz, CDCl<sub>3</sub>):  $\delta$  = 8.91 (s, 1H; *meso*-H), 8.61 (s, 1H; *meso*-H), 4.55 (dd,  $J$  = 3.6, 9.62 Hz, 1H; 17-H), 4.54 (q,  $J$  = 7.2 Hz, 1H; 18-H), 4.23 (m, 2H; N-CH<sub>2</sub>-Hexyl), 3.64 (s, 3H; CO<sub>2</sub>Me), 3.44 (s, 3H; ring-CH<sub>3</sub>), 3.42–3.35 (m, 4H; 3-CH<sub>2</sub>CH<sub>3</sub>, 8-CH<sub>2</sub>CH<sub>3</sub>), 3.08 (s, 3H; ring-CH<sub>3</sub>), 2.92 (s, 3H; ring-CH<sub>3</sub>), 2.66 (t,  $J$  = 8.4 Hz, 2H; 17<sup>2</sup>-CH<sub>2</sub>), 2.42 (m, 1H; 17<sup>1</sup>-CH<sub>2</sub>), 2.04 (m, 1H; 17<sup>1</sup>-CH<sub>2</sub>), 1.82 (m, 2H; CH<sub>2</sub>-Hexyl), 1.52–1.46 (m, 8H; 3-CH<sub>2</sub>CH<sub>3</sub>, 8-CH<sub>2</sub>CH<sub>3</sub>, CH<sub>2</sub>-Hexyl), 1.41–1.35 (m, 4H; 2 CH<sub>2</sub>-Hexyl), 1.18 (d,  $J$  = 7.2 Hz, 3H; 18-CH<sub>3</sub>), 0.91 ppm (t,  $J$  = 7.2 Hz, 3H; CH<sub>3</sub>-Hexyl); <sup>13</sup>C NMR (100 MHz, CDCl<sub>3</sub>):  $\delta$  = 169.8, 162.4, 158.7, 153.0, 145.8, 143.5, 142.5, 139.7, 138.9, 137.0, 135.3, 134.4, 132.2, 131.2, 129.9, 124.9, 124.4, 122.1, 117.0, 104.6, 100.5, 93.2, 88.9, 49.5, 47.6, 46.1, 35.9, 28.2, 27.7, 25.7, 24.8, 23.9, 23.0, 18.7, 15.3, 15.1, 13.6, 13.0, 12.8, 12.2, 10.1, 8.3, 6.6 ppm; UV/Vis (CH<sub>2</sub>Cl<sub>2</sub>):  $\lambda_{\text{max}}$  ( $\epsilon$ ) = 680 nm ( $3.0 \times 10^4 \text{ M}^{-1} \text{ cm}^{-1}$ ); MS (EI):  $m/z$ : 800.0 [M+H]<sup>+</sup>; HRMS: calcd for C<sub>40</sub>H<sub>40</sub>BrN<sub>5</sub>NiO<sub>4</sub>: 797.2087.

**Ni<sup>II</sup> 20-Bromo-N-bis(3,5-trifluoromethyl)benzylmesopurpurin-18-N-hexylimide methyl ester (6):** In a 100 mL dry round-bottomed flask, Ni mesopurpurin-N-bis(trifluoromethyl)benzyl-imide (50.0 mg, 0.058 mmol) was dissolved in dry CH<sub>2</sub>Cl<sub>2</sub> (30.0 mL). N-Bromosuccinimide (12.38 mg, 0.069 mmol) was added to this solution and the resultant mixture was stirred for 30 min at room temperature under N<sub>2</sub>. The progress of the reaction was monitored by UV/Vis spectrophotometry and TLC. After completion of the reaction, saturated sodium bicarbonate (50.0 mL) was gradually added to the reaction mixture and then extracted with dichloromethane (3 × 50.0 mL). The organic layers were collected, combined, and washed with water (100.0 mL). The organic layer was separated, dried over anhydrous Na<sub>2</sub>SO<sub>4</sub>, and concentrated. The crude product was purified through a column of silica by using 1–2% acetone/dichloromethane as eluent. Yield: 40.0 mg (73.3%). <sup>1</sup>H NMR (400 MHz, CDCl<sub>3</sub>):  $\delta$  = 8.94 (s, 1H; *meso*-H), 8.61 (s, 1H; *meso*-H), 8.05 (s, 2H; Ph-H), 7.77 (s, 1H; Ph-H), 5.55 (s, 2H; Benzyl-CH<sub>2</sub>), 4.51–4.47 (m, 2H; 17-H, 18-H), 3.62 (s, 3H; CO<sub>2</sub>Me), 3.45 (s, 3H; ring-CH<sub>3</sub>), 3.42–3.36 (m, 4H; 3-CH<sub>2</sub>CH<sub>3</sub>, 8-CH<sub>2</sub>CH<sub>3</sub>), 3.08 (s, 3H; ring-CH<sub>3</sub>), 2.96 (s, 3H; ring-CH<sub>3</sub>), 2.66–2.63 (m, 2H; 17<sup>2</sup>-CH<sub>2</sub>), 2.22 (m, 1H; 17<sup>1</sup>-CH<sub>2</sub>), 2.02 (m, 1H; 17<sup>1</sup>-CH<sub>2</sub>), 1.53–1.49 (m, 6H; 3-CH<sub>2</sub>CH<sub>3</sub>, 8-CH<sub>2</sub>CH<sub>3</sub>), 1.17 ppm (d,  $J$  = 6.8 Hz, 3H; 18-CH<sub>3</sub>); <sup>13</sup>C NMR (100 MHz, CDCl<sub>3</sub>):  $\delta$  = 173.7, 166.4, 162.3, 162.0, 157.2, 150.0, 148.0, 146.8, 144.0, 143.4, 140.8, 139.3, 138.7, 136.0, 135.4, 134.0, 131.7, 131.4, 128.9, 128.3, 120.0, 109.1, 104.6, 96.5, 93.0, 53.6, 51.5, 50.1, 42.1, 32.1, 29.6, 27.9, 19.2, 19.0, 17.4, 16.9, 16.7, 16.1, 12.4, 10.5 ppm; UV/Vis (CH<sub>2</sub>Cl<sub>2</sub>):  $\lambda_{\text{max}}$  ( $\epsilon$ ) = 683 nm ( $3.3 \times 10^4 \text{ M}^{-1} \text{ cm}^{-1}$ ); MS (EI):  $m/z$ : 964 [M+Na]<sup>+</sup>; HRMS: calcd for C<sub>43</sub>H<sub>38</sub>BrF<sub>6</sub>N<sub>5</sub>NiO<sub>4</sub>: 939.1365; found: 939.1356.

**Ni<sup>II</sup> 20-iodopurpurin-N-hexylimide methyl ester (7):** In a 100 mL dry round-bottomed flask, Ni<sup>II</sup> mesopurpurin-N-hexylimide (50.0 mg, 0.069 mmol) was dissolved in chloroform (30.0 mL). N-Iodosuccinimide

(18.7 mg, 0.083 mmol) and 2 drops of trifluoroacetic acid (TFA) were added and the resultant mixture was stirred for 3–4 min at room temperature under N<sub>2</sub>. The progress of the reaction was monitored by UV/Vis spectrophotometry and TLC. After completion of the reaction, saturated sodium bicarbonate (50.0 mL) was gradually added to the reaction mixture and then extracted with dichloromethane (3 × 50.0 mL). The organic layers were collected, combined, and washed with water (100.0 mL). The organic layer was separated, dried over anhydrous Na<sub>2</sub>SO<sub>4</sub>, and concentrated. The crude product obtained was purified through a column of silica by using 1–2% acetone/dichloromethane as eluent to give compound **7**. Yield: 15.0 mg (25.5%). <sup>1</sup>H NMR (400 MHz, CDCl<sub>3</sub>): δ = 8.88 (s, 1H; *meso*-H), 8.56 (s, 1H; *meso*-H), 4.51 (dd, *J* = 4.0, 9.6 Hz, 1H; 17-H), 4.47 (q, *J* = 6.8 Hz, 1H; 18-H), 4.21 (m, 2H; N-CH<sub>2</sub>-Hexyl), 3.66 (s, 3H; CO<sub>2</sub>Me), 3.43 (s, 3H; ring-CH<sub>3</sub>), 3.41–3.33 (m, 4H; 3-CH<sub>2</sub>CH<sub>3</sub>, 8-CH<sub>2</sub>CH<sub>3</sub>), 3.08 (s, 3H; ring-CH<sub>3</sub>), 2.92 (s, 3H; ring-CH<sub>3</sub>), 2.70–2.65 (m, 2H; 17<sup>2</sup>-CH<sub>2</sub>), 2.27 (m, 1H; 17<sup>1</sup>-CH<sub>2</sub>), 2.09 (m, 1H; 17<sup>1</sup>-CH<sub>2</sub>), 1.81 (m, 2H; CH<sub>2</sub>-Hexyl), 1.51–1.46 (m, 8H; 3-CH<sub>2</sub>CH<sub>3</sub>, 8-CH<sub>2</sub>CH<sub>3</sub>, CH<sub>2</sub>-Hexyl), 1.41–1.34 (m, 4H; 2 CH<sub>2</sub>-Hexyl), 1.12 (d, *J* = 6.8 Hz, 3H; 18-CH<sub>3</sub>), 0.90 ppm (t, *J* = 7.2 Hz, 3H; CH<sub>3</sub>-Hexyl); <sup>13</sup>C NMR (100 MHz, CDCl<sub>3</sub>): δ = 173.8, 166.2, 162.2, 158.9, 150.1, 149.4, 146.7, 143.5, 143.1, 141.0, 139.4, 138.0, 136.3, 135.2, 133.7, 121.1, 108.8, 104.7, 62.3, 54.2, 53.7, 51.6, 39.8, 32.3, 31.6, 29.6, 29.3, 28.7, 27.3, 27.0, 22.6, 19.4, 19.0, 17.3, 16.9, 14.1, 12.2, 10.4 ppm; UV/Vis (CH<sub>2</sub>Cl<sub>2</sub>): λ<sub>max</sub> (ε) = 685 nm (3.4 × 10<sup>4</sup> M<sup>-1</sup> cm<sup>-1</sup>); MS (EI): *m/z*: 870 [M+Na]<sup>+</sup>; HRMS: calcd for C<sub>40</sub>H<sub>46</sub>N<sub>3</sub>NiO<sub>4</sub>: 845.1948; found: 845.1953.

**Ni<sup>II</sup> meso-Purpurin-N-hexylimide-emeraldine (8)**: Yield: 10.0 mg (20.0%). <sup>1</sup>H NMR (400 MHz, CDCl<sub>3</sub>): δ = 9.24 (s, 1H; *meso*-H), 9.04 (s, 1H; *meso*-H), 8.97 (s, 1H; *meso*-H), 4.37 (t, *J* = 7.6 Hz, 2H; N-CH<sub>2</sub>-Hexyl), 3.90 (t, *J* = 7.6 Hz, 2H; 17<sup>1</sup>-CH<sub>2</sub>), 3.72 (s, 3H; CO<sub>2</sub>Me), 3.67 (s, 3H; ring-CH<sub>3</sub>), 3.57 (m, 4H; 3-CH<sub>2</sub>CH<sub>3</sub>, 8-CH<sub>2</sub>CH<sub>3</sub>), 3.17 (t, *J* = 8.4 Hz, 3H; 17<sup>2</sup>-CH<sub>2</sub>), 3.16 (s, 3H; ring-CH<sub>3</sub>), 3.15 (s, 3H; ring-CH<sub>3</sub>), 3.14 (s, 3H; ring-CH<sub>3</sub>), 1.99 (m, 2H; CH<sub>2</sub>-Hexyl), 1.65–1.63 (m, 2H; CH<sub>2</sub>-Hexyl), 1.56 (m, 6H; 3-CH<sub>2</sub>CH<sub>3</sub>, 8-CH<sub>2</sub>CH<sub>3</sub>), 1.51–1.42 (m, 4H; 2 CH<sub>2</sub>-Hexyl), 0.96 ppm (t, *J* = 7.2 Hz, 3H; CH<sub>3</sub>-Hexyl); <sup>13</sup>C NMR (100 MHz, CDCl<sub>3</sub>): δ = 173.9, 166.2, 163.1, 146.9, 145.4, 144.4, 143.2, 142.6, 142.4, 142.2, 141.1, 140.8, 140.4, 138.7, 136.9, 136.7, 136.5, 125.5, 101.7, 99.8, 98.7, 98.3, 51.5, 40.1, 36.3, 31.7, 29.6, 29.0, 27.1, 24.1, 22.7, 19.4, 19.3, 17.2, 14.1, 12.5, 11.7, 11.1, 11.0 ppm; UV/Vis (CH<sub>2</sub>Cl<sub>2</sub>): λ<sub>max</sub> (ε) = 647 nm (1.5 × 10<sup>4</sup> M<sup>-1</sup> cm<sup>-1</sup>); MS (EI): *m/z*: 719 [M+H]<sup>+</sup>; HRMS: calcd for C<sub>40</sub>H<sub>45</sub>N<sub>3</sub>NiO<sub>4</sub>: 717.2825; found: 717.2300.

**Ni<sup>II</sup> Bis(3,5-trifluoromethyl)benzylemeraldine methyl ester (9)**: In a 100 mL dry round-bottomed flask, Ni<sup>II</sup> mesopurpurin-N-hexylimide (50.0 mg, 0.058 mmol) was dissolved in chloroform (30.0 mL). *N*-Iodosuccinimide (15.6 mg, 0.069 mmol) and 2 drops of TFA were added and the resultant mixture was stirred for 3–4 min at room temperature under N<sub>2</sub>. The progress of the reaction was monitored by UV/Vis spectrophotometry and TLC. After completion of the reaction, saturated sodium bicarbonate (50.0 mL) was gradually added to the reaction mixture and then extracted with dichloromethane (3 × 50.0 mL). The organic layers were collected, combined, and washed with water (100.0 mL). The organic layer was separated, dried over anhydrous Na<sub>2</sub>SO<sub>4</sub>, and concentrated. The crude thus obtained was purified through a column of silica by using 1–2% acetone/dichloromethane as eluent. Yield: 25.0 mg (50.2%). <sup>1</sup>H NMR (400 MHz, CDCl<sub>3</sub>): δ = 9.38 (s, 1H; *meso*-H), 9.15 (s, 1H; *meso*-H), 9.14 (s, 1H; *meso*-H), 8.19 (s, 2H; Ph-H), 7.81 (s, 1H; Ph-H), 5.65 (s, 2H; Benzyl-CH<sub>2</sub>), 3.83 (t, *J* = 7.6 Hz, 2H; 17<sup>1</sup>-CH<sub>2</sub>), 3.72 (s, 3H; CO<sub>2</sub>Me), 3.65–3.61 (m, 4H; 3-CH<sub>2</sub>CH<sub>3</sub>, 8-CH<sub>2</sub>CH<sub>3</sub>), 3.57 (s, 3H; ring-CH<sub>3</sub>), 3.21 (s, 3H; ring-CH<sub>3</sub>), 3.19 (s, 3H; ring-CH<sub>3</sub>), 3.17 (s, 3H; ring-CH<sub>3</sub>), 2.98 (t, *J* = 7.2 Hz, 2H; 17<sup>2</sup>-CH<sub>2</sub>), 1.64–1.59 ppm (m, 6H; 3-CH<sub>2</sub>CH<sub>3</sub>, 8-CH<sub>2</sub>CH<sub>3</sub>); <sup>13</sup>C NMR (100 MHz, CDCl<sub>3</sub>): δ = 189.9, 173.5, 166.2, 162.8, 148.0, 146.1, 145.2, 145.0, 144.0, 143.4, 142.8, 141.7, 141.3, 140.9, 139.0, 137.6, 137.2, 131.8, 129.1, 125.1, 102.6, 100.6, 99.3, 97.5, 69.7, 51.4, 42.6, 36.0, 31.9, 29.7, 29.3, 24.3, 24.0, 22.7, 19.5, 17.3, 14.1, 12.8, 11.9, 11.2 ppm; UV/Vis (CH<sub>2</sub>Cl<sub>2</sub>): λ<sub>max</sub> (ε) = 655 nm (1.6 × 10<sup>4</sup> M<sup>-1</sup> cm<sup>-1</sup>); MS (EI): *m/z*: 861 [M+H]<sup>+</sup>; HRMS: calcd for C<sub>43</sub>H<sub>37</sub>F<sub>6</sub>N<sub>3</sub>NiO<sub>4</sub>: 859.2103; found: 859.2101.

**Ni<sup>II</sup> 20-methylmesopurpurin-18-N-hexylimide methyl ester (10)**: In a dry round-bottomed flask (100 mL), Ni<sup>II</sup> 20-bromo-N-hexylmesopurpurin-

nimide (50.0 mg, 0.062 mmol), Cs<sub>2</sub>CO<sub>3</sub> (20.16 mg, 0.062 mmol), methyl boronic acid pinacol ester (88 mg, 0.62 mmol), and 1,1'-bis(diphenylphosphino)ferrocenepalladium(II) chloride ([PdCl<sub>2</sub>(dppf)]): 9.06 mg, 0.0124 mmol) were dissolved in dry THF (35 mL). The resultant mixture was heated at reflux for 12 h. The progress of the reaction was monitored by UV/Vis spectrophotometry and TLC. After completion of the reaction, the mixture was taken up in CH<sub>2</sub>Cl<sub>2</sub> (100 mL) and washed with brine. The organic layer was separated and dried over sodium sulfate. The crude residue obtained was purified by chromatography through a column of silica gel by using 0.5–1% acetone/CH<sub>2</sub>Cl<sub>2</sub> to obtain product **10** in good yield. Yield: 38.0 mg (84.2%). <sup>1</sup>H NMR (400 MHz, CDCl<sub>3</sub>): δ = 8.91 (s, 1H; *meso*-H), 8.57 (s, 1H; *meso*-H), 4.58 (dd, *J* = 4.0, 9.2 Hz, 1H; 17-H), 4.26–4.21 (m, 2H; N-CH<sub>2</sub>-Hexyl), 4.08 (q, *J* = 6.8 Hz, 1H; 18-H), 3.64 (s, 3H; CO<sub>2</sub>Me), 3.46 (s, 3H; ring-CH<sub>3</sub>), 3.43–3.35 (m, 4H; 8-CH<sub>2</sub>CH<sub>3</sub>, 3-CH<sub>2</sub>CH<sub>3</sub>), 2.99 (s, 3H; ring-CH<sub>3</sub>), 2.97 (s, 3H; ring-CH<sub>3</sub>), 2.95 (s, 3H; ring-CH<sub>3</sub>), 2.66–2.61 (m, 2H; 17<sup>2</sup>-CH<sub>2</sub>), 2.20 (m, 1H; 17<sup>1</sup>-CHH), 2.00 (m, 1H; 17<sup>1</sup>-CHH), 1.85–1.82 (m, 2H; CH<sub>2</sub>-Hexyl), 1.56–1.53 (m, 2H; CH<sub>2</sub>-Hexyl), 1.51–1.48 (m, 6H; 8-CH<sub>2</sub>CH<sub>3</sub>, 3-CH<sub>2</sub>CH<sub>3</sub>), 1.43–1.33 (m, 4H; 2 CH<sub>2</sub>-Hexyl), 1.13 (d, *J* = 6.8 Hz, 3H; 18-CH<sub>3</sub>), 0.91 ppm (t, *J* = 6.8 Hz, 3H; CH<sub>3</sub>-Hexyl); <sup>13</sup>C NMR (100 MHz, CDCl<sub>3</sub>): δ = 174.0, 166.7, 162.9, 160.0, 156.4, 150.2, 149.2, 145.3, 143.2, 142.9, 140.5, 138.8, 138.7, 135.7, 133.9, 133.0, 120.3, 108.1, 104.0, 103.0, 96.6, 54.0, 51.5, 45.6, 39.8, 32.2, 31.7, 28.8, 27.6, 27.0, 22.7, 19.0, 18.8, 17.9, 17.0, 16.8, 15.2, 14.0, 12.2, 10.5 ppm; UV/Vis (CH<sub>2</sub>Cl<sub>2</sub>): λ<sub>max</sub> (ε) = 677 nm (3.1 × 10<sup>4</sup> M<sup>-1</sup> cm<sup>-1</sup>); MS (EI): *m/z*: 757 [M+Na]<sup>+</sup>; HRMS: calcd for C<sub>41</sub>H<sub>49</sub>N<sub>3</sub>NiO<sub>4</sub>: 733.3138; found: 733.3180.

**Ni<sup>II</sup> 20-(tert-butyl)dimethylsilylacetylenylmesopurpurin-18-N-hexylimide methyl ester (11)**: In a dry round-bottomed flask (50 mL), Ni<sup>II</sup> 20-bromo-N-hexylmesopurpurinimide (25.0 mg, 0.032 mmol), Cs<sub>2</sub>CO<sub>3</sub> (10 mg, 0.032 mmol), *tert*-butyldimethylsilylacetylenylboronic acid (58 mg, 0.32 mmol), and [PdCl<sub>2</sub>(dppf)] (4.6 mg, 0.0064 mmol) were dissolved in dry THF (15 mL). The resultant mixture was heated at reflux for 12 h. The progress of the reaction was monitored by UV/Vis spectrophotometry and TLC. After completion of the reaction, the mixture was taken up in CH<sub>2</sub>Cl<sub>2</sub> (50 mL) and washed with brine. The organic layer was separated and dried over sodium sulfate. The crude residue obtained was purified by chromatography through a column of silica gel by using 0.5–1% acetone/CH<sub>2</sub>Cl<sub>2</sub> to obtain product **11** in good yield. Yield: 15.6 mg (57%). <sup>1</sup>H NMR (400 MHz, CDCl<sub>3</sub>): δ = 8.89 (s, 1H; *meso*-H), 8.55 (s, 1H; *meso*-H), 4.58 (dd, *J* = 4.0, 9.2 Hz, 1H; 17-H), 4.50 (q, *J* = 7.2 Hz, 1H; 18-H), 4.19–4.27 (m, 2H; N-CH<sub>2</sub>-Hexyl), 3.61 (s, 3H; CO<sub>2</sub>Me), 3.44 (s, 3H; ring-CH<sub>3</sub>), 3.33–3.40 (m, 4H; 8-CH<sub>2</sub>CH<sub>3</sub>, 3-CH<sub>2</sub>CH<sub>3</sub>), 3.12 (s, 3H; ring-CH<sub>3</sub>), 2.92 (s, 3H; ring-CH<sub>3</sub>), 2.58 (t, *J* = 7.2 Hz, 2H; 17<sup>2</sup>-CH<sub>2</sub>), 2.16–2.20 (m, 1H; 17<sup>1</sup>-CHH), 1.90–1.96 (m, 1H; 17<sup>1</sup>-CHH), 1.82 (m, 2H; CH<sub>2</sub>-Hexyl), 1.49–1.52 (m, 8H; CH<sub>2</sub>-Hexyl, 8-CH<sub>2</sub>CH<sub>3</sub>, 3-CH<sub>2</sub>CH<sub>3</sub>), 1.42–1.46 (m, 4H; 2 CH<sub>2</sub>-Hexyl), 1.26 (d, *J* = 6.8 Hz, 3H; 18-CH<sub>3</sub>), 1.07 (s, 9H; Si-*tert*-Bu), 0.91 (t, *J* = 6.8 Hz, 3H; CH<sub>3</sub>-Hexyl), 0.30 (s, 3H; Si-Me), 0.28 ppm (s, 3H; Si-Me); <sup>13</sup>C NMR (100 MHz, CDCl<sub>3</sub>): δ = 173.7, 166.5, 164.4, 162.7, 161.4, 149.3, 148.7, 145.4, 143.8, 143.5, 141.0, 138.8, 138.7, 135.6, 135.2, 133.4, 126.4, 120.0, 109.1, 104.5, 103.5, 102.5, 98.4, 92.1, 53.0, 51.5, 48.4, 45.7, 39.9, 31.9, 31.7, 28.8, 28.4, 27.0, 26.2, 22.7, 19.1, 18.2, 17.1, 17.0, 16.8, 14.4, 14.1, 12.1, 10.6, –4.6 ppm; UV/Vis (CH<sub>2</sub>Cl<sub>2</sub>): λ<sub>max</sub> (ε) = 670 nm (3.0 × 10<sup>4</sup> M<sup>-1</sup> cm<sup>-1</sup>); MS (EI): *m/z*: 858 [M+H]<sup>+</sup>; HRMS: calcd for C<sub>48</sub>H<sub>61</sub>N<sub>3</sub>NiO<sub>4</sub>Si-H: 858.3919; found: 858.3916.

**Ni<sup>II</sup> 20-(6-dimethylaminopyridin-3-yl)mesopurpurin-18-N-hexylimide methyl ester (12)**: Compound **12** was prepared by following the experimental procedure for compound **10**. Yield: 35.0 mg (67.8%). <sup>1</sup>H NMR (400 MHz, CDCl<sub>3</sub>): δ = 8.98 (s, 1H; *meso*-H), 8.64 (s, 1H; *meso*-H), 8.97, 8.26 (s, d, *J* = 8.2 Hz, 1H; Py-H), 7.49, 6.88 (s, d, *J* = 9.6 Hz, 1H; Py-H), 6.76, 6.48 (d, d, *J* = 8.8, 8.8 Hz, 1H; Py-H), 4.52 (m, 1H; 17-H), 4.29–4.21 (m, 2H; N-CH<sub>2</sub>-Hexyl), 4.12, 3.74 (q, *J* = 7.2 Hz, 1H; 18-H), 3.67 (s, 3H; CO<sub>2</sub>Me), 3.48 (s, 3H; ring-CH<sub>3</sub>), 3.45–3.39 (m, 2H; 8-CH<sub>2</sub>CH<sub>3</sub>), 3.38–3.33 (m, 2H; 3-CH<sub>2</sub>CH<sub>3</sub>), 3.23 (s, 3H; *Me*-*N*-Me), 3.21 (s, 3H; *Me*-*N*-Me), 2.97 (s, 3H; ring-CH<sub>3</sub>), 2.69 (t, *J* = 8.0 Hz, 2H; 17<sup>2</sup>-CH<sub>2</sub>), 2.31 (m, 1H; 17<sup>1</sup>-CHH), 2.15 (m, 1H; 17<sup>1</sup>-CHH), 2.08, 2.07 (s, 3H; ring-CH<sub>3</sub>), 1.83 (m, 2H; -CH<sub>2</sub>-Hexyl), 1.50 (t, *J* = 7.6 Hz, 3H; 8-CH<sub>2</sub>CH<sub>3</sub>), 1.47 (m, 2H; -CH<sub>2</sub>-Hexyl), 1.45 (t, *J* = 7.6 Hz, 3H; 3-CH<sub>2</sub>CH<sub>3</sub>), 1.38–1.36 (m, 4H; 2 CH<sub>2</sub>-Hexyl), 0.90 (t, *J* = 6.8 Hz, 3H; CH<sub>3</sub>-Hexyl), 0.73 ppm (d, *J* = 6.4 Hz, 3H; 18-CH<sub>3</sub>); <sup>13</sup>C NMR (100 MHz, CDCl<sub>3</sub>, mixture of topoisomers): δ =

174.0, 173.7, 166.8, 162.9, 161.5, 161.0, 158.8, 149.3, 149.0, 145.5, 143.6, 143.5, 143.2, 143.1, 140.7, 139.1, 138.6, 135.7, 135.2, 133.3, 127.8, 123.0, 122.8, 120.3, 114.6, 108.4, 103.2, 97.3, 53.5, 51.6, 45.1, 39.8, 32.5, 32.5, 32.4, 31.6, 29.6, 29.2, 28.8, 27.6, 27.0, 22.7, 19.0, 18.1, 17.0, 16.7, 14.6, 14.3, 14.0, 12.3, 10.6 ppm; UV/Vis (CH<sub>2</sub>Cl<sub>2</sub>):  $\lambda_{\max}$  ( $\epsilon$ ) = 677 nm ( $3.2 \times 10^4 \text{ M}^{-1} \text{ cm}^{-1}$ ); MS (EI):  $m/z$ : 840 [M]<sup>+</sup>, 862 [M+Na]<sup>+</sup>; HRMS: calcd for C<sub>47</sub>H<sub>55</sub>N<sub>7</sub>NiO<sub>4</sub>: 839.3669; found: 839.3672.

**Ni<sup>II</sup> 20-(4-aminophenyl)mesopurpurin-18-N-hexylimide methyl ester (14):** Compound **14** was prepared by following the experimental procedure for compound **11**. Yield: 15.7 mg (60%). <sup>1</sup>H NMR (400 MHz, CDCl<sub>3</sub>):  $\delta$  = 8.99 (s, 1H; *meso*-H), 8.65 (s, 1H; *meso*-H), 7.97 (d,  $J$  = 8.2 Hz, 1H; Ar-H), 7.05 (d,  $J$  = 9.6 Hz, 1H; Ar-H), 6.66 (d,  $J$  = 8.8 Hz, 1H; Ar-H), 6.51 (d,  $J$  = 8.8 Hz, 1H; Ar-H), 4.51 (m, 1H; 17-H), 4.22–4.29 (m, 3H; N-CH<sub>2</sub>-Hexyl, 18-H), 3.47 (brs, 2H; NH<sub>2</sub>), 3.77 (s, 3H; CO<sub>2</sub>Me), 3.50 (s, 3H; ring-CH<sub>3</sub>), 3.30–3.50 (m, 4H; 8-CH<sub>2</sub>CH<sub>3</sub>, 3-CH<sub>2</sub>CH<sub>3</sub>), 2.99 (s, 3H; ring-CH<sub>3</sub>), 2.69 (t,  $J$  = 8.0 Hz, 2H; 17<sup>2</sup>-CH<sub>2</sub>), 2.32–2.35 (m, 1H; 17<sup>1</sup>-CHH), 2.14–2.18 (m, 1H; 17<sup>1</sup>-CHH), 2.04 (s, 3H; ring-CH<sub>3</sub>), 1.83–1.89 (m, 2H; CH<sub>2</sub>-Hexyl), 1.27–1.55 (m, 12H; 8-CH<sub>2</sub>CH<sub>3</sub>, 3-CH<sub>2</sub>CH<sub>3</sub>, 3 CH<sub>2</sub>-Hexyl), 0.93 (t,  $J$  = 6.8 Hz, 3H; CH<sub>3</sub>-Hexyl), 0.72 ppm (d,  $J$  = 6.4 Hz, 3H; 18-CH<sub>3</sub>); <sup>13</sup>C NMR (100 MHz, CDCl<sub>3</sub>):  $\delta$  = 173.7, 166.6, 164.9, 162.8, 162.3, 152.7, 149.2, 148.2, 147.6, 144.7, 141.7, 138.4, 138.8, 136.3, 135.0, 134.9, 134.6, 131.5, 119.6, 113.1, 109.3, 100.4, 100.1, 98.0, 95.0, 83.7, 52.8, 51.5, 48.0, 47.5, 40.1, 31.9, 31.6, 28.9, 28.7, 28.3, 27.0, 24.8, 22.6, 20.9, 19.0, 16.8, 16.7, 16.4, 14.0, 10.6 ppm; UV/Vis (CH<sub>2</sub>Cl<sub>2</sub>):  $\lambda_{\max}$  ( $\epsilon$ ) = 676 nm ( $3.2 \times 10^4 \text{ M}^{-1} \text{ cm}^{-1}$ ); MS (EI):  $m/z$ : 833.6 [M+Na]<sup>+</sup>; HRMS: calcd for C<sub>40</sub>H<sub>52</sub>N<sub>6</sub>NiO<sub>4</sub>+H: 811.3476; found: 811.3470.

**Ni<sup>II</sup> 20-(3-aminophenyl)mesopurpurin-18-N-hexylimide methyl ester (15):** Compound **15** was prepared by following the experimental procedure for compound **11**. Yield: 15.2 mg (59%). <sup>1</sup>H NMR (400 MHz, CDCl<sub>3</sub>, mixture of both topoisomers):  $\delta$  = 8.97, 9.40 (s, 1H; *meso*-H), 8.64, 8.63 (s, 1H; *meso*-H), 7.58–7.60 (m, 0.95H; Ar-H), 7.48 (t,  $J$  = 7.8 Hz, 0.40H; Ar-H), 7.11 (t,  $J$  = 7.2 Hz, 0.55H; Ar-H), 6.80–6.85 (m, 0.8H; Ar-H), 6.20 (d,  $J$  = 7.2 Hz, 0.40H; Ar-H), 6.07 (s, 0.35H; Ar-H), 4.42–4.62 (m, 1H; 17-H), 4.22–4.32 (m, 3H; N-CH<sub>2</sub>-Hexyl, 18-H), 3.71, 3.68 (s, 3H; CO<sub>2</sub>Me), 3.52 (s, 3H; ring-CH<sub>3</sub>), 3.31–3.57 (m, 4H; 8-CH<sub>2</sub>CH<sub>3</sub>, 3-CH<sub>2</sub>CH<sub>3</sub>), 2.97, 2.95 (s, 3H; ring-CH<sub>3</sub>), 2.63–2.70 (m, 2H; 17<sup>2</sup>-CH<sub>2</sub>), 2.32–2.38 (m, 1H; 17<sup>1</sup>-CHH), 2.06–2.20 (m, 1H; 17<sup>1</sup>-CHH, 3H; ring-CH<sub>3</sub>), 1.80–1.86 (m, 2H; CH<sub>2</sub>-Hexyl), 1.22–1.61 (m, 12H; 8-CH<sub>2</sub>CH<sub>3</sub>, 3-CH<sub>2</sub>CH<sub>3</sub>, 3 CH<sub>2</sub>-Hexyl), 0.91 (t,  $J$  = 6.8 Hz, 3H; CH<sub>3</sub>-Hexyl), 0.78, 0.76 ppm (d,  $J$  = 6.6 Hz, 3H; 18-CH<sub>3</sub>); <sup>13</sup>C NMR (100 MHz, CDCl<sub>3</sub>, mixture of both topoisomers):  $\delta$  = 196.2, 173.4, 171.9, 156.1, 148.3, 144.4, 141.5, 141.1, 140.0, 139.6, 138.9, 136.7, 134.5, 134.3, 133.9, 133.6, 133.1, 133.0, 132.2, 132.1, 131.0, 127.2, 126.6, 115.4, 103.5, 98.7, 72.8, 69.6, 69.4, 52.0, 51.6, 48.6, 48.2, 44.6, 31.7, 31.6, 31.1, 30.2, 30.0, 29.8, 28.3, 26.0, 24.9, 24.5, 22.5, 21.0, 19.4, 17.3, 13.9, 13.8, 13.7, 13.4, 12.1, 11.3 ppm; UV/Vis (CH<sub>2</sub>Cl<sub>2</sub>):  $\lambda_{\max}$  ( $\epsilon$ ) = 675 nm ( $3.0 \times 10^4 \text{ M}^{-1} \text{ cm}^{-1}$ ); MS (EI):  $m/z$ : 833.6 [M+Na]<sup>+</sup>; HRMS: calcd for C<sub>40</sub>H<sub>52</sub>N<sub>6</sub>NiO<sub>4</sub>+H: 811.3476; found: 811.3487.

**Ni<sup>II</sup> 20-(4-tert-butoxycarbonylphenyl)mesopurpurin-18-N-hexylimide methyl ester (16):** Compound **16** was prepared by following the experimental procedure for compound **11**. Yield: 18.6 mg (65%). <sup>1</sup>H NMR (400 MHz, CDCl<sub>3</sub>):  $\delta$  = 9.00 (s, 1H; *meso*-H), 8.68 (s, 1H; *meso*-H), 8.48 (d,  $J$  = 8.2 Hz, 1H; Ar-H), 8.39 (d,  $J$  = 9.6 Hz, 1H; Ar-H), 7.90 (d,  $J$  = 8.8 Hz, 1H; Ar-H), 6.89 (d,  $J$  = 8.8 Hz, 1H; Ar-H), 5.50 (dd,  $J$  = 4.0, 9.2 Hz, 1H; 17-H), 4.20–4.25 (m, 2H; N-CH<sub>2</sub>-Hexyl), 4.10–4.14 (m, 1H; 18-H), 3.68 (s, 3H; CO<sub>2</sub>Me), 3.49 (s, 3H; ring-CH<sub>3</sub>), 3.26–3.45 (m, 4H; 8-CH<sub>2</sub>CH<sub>3</sub>, 3-CH<sub>2</sub>CH<sub>3</sub>), 2.99 (s, 3H; ring-CH<sub>3</sub>), 2.63–2.71 (m, 2H; 17<sup>2</sup>-CH<sub>2</sub>), 2.31–2.34 (m, 1H; 17<sup>1</sup>-CHH), 2.13–2.18 (m, 1H; 17<sup>1</sup>-CHH), 1.91 (s, 3H; ring-CH<sub>3</sub>), 1.82 (m, 2H; CH<sub>2</sub>-Hexyl), 1.20–1.67 (m, 21H; 8-CH<sub>2</sub>CH<sub>3</sub>, 3 CH<sub>2</sub>-Hexyl, 3-CH<sub>2</sub>CH<sub>3</sub>, *t*-Butyl), 0.90 (t,  $J$  = 6.8 Hz, 3H; CH<sub>3</sub>-Hexyl), 0.67 ppm (d,  $J$  = 6.4 Hz, 3H; 18-CH<sub>3</sub>); <sup>13</sup>C NMR (100 MHz, CDCl<sub>3</sub>):  $\delta$  = 189.9, 173.8, 166.2, 165.7, 161.8, 161.6, 150.5, 150.0, 148.4, 147.8, 143.1, 141.9, 137.8, 137.2, 135.0, 134.5, 134.2, 132.3, 131.8, 129.3, 128.3, 120.6, 113.3, 111.4, 101.5, 99.8, 84.0, 81.5, 81.0, 53.3, 51.6, 45.7, 40.1, 32.3, 31.6, 28.7, 28.1, 27.8, 26.9, 24.8, 22.6, 19.0, 18.9, 18.2, 16.7, 16.4, 14.0, 13.9, 10.5 ppm; UV/Vis (CHCl<sub>3</sub>):  $\lambda_{\max}$  ( $\epsilon$ ) = 672 nm ( $3.2 \times 10^4 \text{ M}^{-1} \text{ cm}^{-1}$ ); MS (EI):  $m/z$ : 896 [M+H]<sup>+</sup>; HRMS: calcd for C<sub>51</sub>H<sub>59</sub>N<sub>5</sub>NiO<sub>6</sub>+H: 896.3892; found: 896.4222.

**Ni<sup>II</sup> 20-(3-carboxyphenyl)mesopurpurin-18-N-hexylimide methyl ester (17):** Compound **17** was prepared by following the experimental procedure for compound **11**. Yield: 12 mg (45%). <sup>1</sup>H NMR (400 MHz, CDCl<sub>3</sub>, mixture of both topoisomers)  $\delta$  = 10.09, 9.84 (s, 1H; COOH), 8.93 (s, 1H; *meso*-H), 8.63 (s, 1H; *meso*-H), 8.11, 7.66 (s, 1H; Ar-H), 8.06, 7.35 (d,  $J$  = 7.6, 1H, Ar-H), 7.88 (m, 1H; Ar-H), 7.51–7.68 (m, 1H; Ar-H) 4.56 (m, 1H; 17-H), 4.50 (m, 1H; 18-H), 4.23 (m, 2H; N-CH<sub>2</sub>-Hexyl), 3.64 (s, 3H; CO<sub>2</sub>Me), 3.44 (s, 3H; ring-CH<sub>3</sub>), 3.36–3.44 (m, 4H; 3-CH<sub>2</sub>CH<sub>3</sub>, 8-CH<sub>2</sub>CH<sub>3</sub>), 3.09 (s, 3H; ring-CH<sub>3</sub>), 3.87 (s, 3H; ring-CH<sub>3</sub>), 2.67–2.69 (m, 2H; 17<sup>2</sup>-CH<sub>2</sub>), 2.24 (m, 1H; 17<sup>1</sup>-CHH), 2.04 (m, 1H; 17<sup>1</sup>-CHH), 1.42–1.53 (m, 10H; CH<sub>2</sub>-Hexyl, CH<sub>2</sub>-Hexyl, 8-CH<sub>2</sub>CH<sub>3</sub>, 3-CH<sub>2</sub>CH<sub>3</sub>), 1.34–1.40 (m, 4H; 2 CH<sub>2</sub>-Hexyl), 1.18 (d,  $J$  = 6.8 Hz, 3H; 18-CH<sub>3</sub>), 0.88 ppm (t,  $J$  = 7.2 Hz, 3H; CH<sub>3</sub>-Hexyl); UV/Vis (CHCl<sub>3</sub>):  $\lambda_{\max}$  ( $\epsilon$ ) = 671 nm ( $3.3 \times 10^4 \text{ M}^{-1} \text{ cm}^{-1}$ ); MS (EI):  $m/z$ : 862 [M+Na]<sup>+</sup>; HRMS: calcd for C<sub>50</sub>H<sub>51</sub>N<sub>5</sub>NiO<sub>6</sub>: 839.3193; found: 839.3277.

**Ni<sup>II</sup> 20-(4-carboxyphenyl)mesopurpurin-18-N-hexylimide methyl ester (17a):** Compound **17a** was prepared by following the experimental procedure for compound **11**. Yield: approx. 2 mg (5%). <sup>1</sup>H NMR (400 MHz, CDCl<sub>3</sub>):  $\delta$  = 9.52 (s, 1H; *meso*-H), 9.30 (d,  $J$  = 8.0 Hz, 1H; ArH), 8.98 (s, 1H; *meso*-H), 8.56 (d,  $J$  = 8.6 Hz, 1H; Ar-H), 8.11 (d,  $J$  = 8.0 Hz, 1H; Ar-H), 7.68 (d,  $J$  = 8.8 Hz, 1H; Ar-H), 4.60 (dd,  $J$  = 4.3, 9.0 Hz, 1H; 17-H), 4.16–4.22 (m, 2H; N-CH<sub>2</sub>-Hexyl), 3.94–4.04 (m, 1H; 18-H), 3.55 (s, 3H; CO<sub>2</sub>Me), 3.41 (s, 3H; ring-CH<sub>3</sub>), 3.26–3.34 (m, 4H; 8-CH<sub>2</sub>CH<sub>3</sub>, 3-CH<sub>2</sub>CH<sub>3</sub>), 2.94 (s, 3H; ring-CH<sub>3</sub>), 2.81 (s, 3H; ring-CH<sub>3</sub>), 2.43–2.61 (m, 2H; 17<sup>2</sup>-CH<sub>2</sub>), 2.04–2.23 (m, 1H; 17<sup>1</sup>-CHH), 1.69–1.88 (m, 1H; 17<sup>1</sup>-CHH), 1.22–1.51 (m, 17H; CH<sub>2</sub>-Hexyl, 18-CH<sub>3</sub>, 8-CH<sub>2</sub>CH<sub>3</sub>, 3 CH<sub>2</sub>-Hexyl, 3-CH<sub>2</sub>CH<sub>3</sub>), 0.82 ppm (t,  $J$  = 6.8 Hz, 3H; CH<sub>3</sub>-Hexyl); <sup>13</sup>C NMR (100 MHz, CDCl<sub>3</sub>):  $\delta$  = 189.8, 174.2, 166.1, 162.1, 161.7, 161.3, 150.2, 149.7, 148.3, 147.8, 142.8, 141.9, 137.7, 136.9, 135.1, 134.6, 132.3, 131.8, 129.8, 120.5, 113.2, 111.5, 105.0, 101.4, 99.8, 53.1, 51.6, 45.7, 40.0, 32.4, 31.8, 31.5, 29.6, 29.3, 28.6, 27.8, 26.9, 22.6, 22.5, 18.9, 18.5, 18.2, 16.7, 16.1, 14.0, 13.6, 10.4 ppm; UV/Vis (CHCl<sub>3</sub>):  $\lambda_{\max}$  ( $\epsilon$ ) = 672 nm ( $3.2 \times 10^4 \text{ M}^{-1} \text{ cm}^{-1}$ ); MS (EI):  $m/z$ : 862 [M+Na]<sup>+</sup>; HRMS: calcd for C<sub>50</sub>H<sub>51</sub>N<sub>5</sub>NiO<sub>6</sub>: 839.3193; found: 839.3166.

**Ni<sup>II</sup> 20-(4-formylphenyl)mesopurpurin-18-N-hexylimide methyl ester (18):** Compound **18** was prepared by following the experimental procedure for compound **11**. Yield: 20.3 mg (77%). <sup>1</sup>H NMR (400 MHz, CDCl<sub>3</sub>):  $\delta$  = 10.19 (s, 1H; CHO), 9.00 (s, 1H; *meso*-H), 8.69 (s, 1H; *meso*-H), 8.49 (d,  $J$  = 8.0 Hz, 1H; Ph-H), 8.28 (d,  $J$  = 7.6 Hz, 1H; Ph-H), 7.88 (d,  $J$  = 7.2 Hz, 1H; Ph-H), 6.96 (d,  $J$  = 7.2 Hz, 1H; Ph-H), 4.51 (dd,  $J$  = 3.6, 9.2 Hz, 1H; 17-H), 4.24 (m, 2H; N-CH<sub>2</sub>-Hexyl), 4.11 (q,  $J$  = 6.8 Hz, 1H; 18-H), 3.68 (s, 3H; CO<sub>2</sub>Me), 3.49 (s, 3H; ring-CH<sub>3</sub>), 3.42–3.48 (m, 2H; 8-CH<sub>2</sub>CH<sub>3</sub>), 3.29–3.41 (m, 2H; 3-CH<sub>2</sub>CH<sub>3</sub>), 2.98 (s, 3H; ring-CH<sub>3</sub>), 2.66–2.71 (m, 2H; 17<sup>2</sup>-CH<sub>2</sub>), 2.33 (m, 1H; 17<sup>1</sup>-CHH), 2.18 (m, 1H; 17<sup>1</sup>-CHH), 1.90 (s, 3H; ring-CH<sub>3</sub>), 1.83 (m, 2H; CH<sub>2</sub>-Hexyl), 1.54–1.56 (m, 2H; CH<sub>2</sub>-Hexyl), 1.52 (t,  $J$  = 7.6 Hz, 3H; 8-CH<sub>2</sub>CH<sub>3</sub>), 1.45 (t,  $J$  = 6.8 Hz, 3H; 3-CH<sub>2</sub>CH<sub>3</sub>), 1.33–1.37 (m, 4H; 2 CH<sub>2</sub>-Hexyl), 0.91 (t,  $J$  = 7.2 Hz, 3H; CH<sub>3</sub>-Hexyl), 0.68 ppm (d,  $J$  = 6.8 Hz, 3H; 18-CH<sub>3</sub>); <sup>13</sup>C NMR (100 MHz, CDCl<sub>3</sub>):  $\delta$  = 191.8, 173.9, 166.6, 162.8, 161.2, 156.8, 149.3, 147.8, 146.3, 146.0, 143.7, 143.0, 141.1, 138.9, 138.8, 136.0, 135.6, 134.2, 133.6, 133.3, 132.7, 129.4, 120.6, 114.0, 110.4, 108.5, 103.9, 97.4, 53.7, 51.6, 45.0, 39.8, 32.5, 31.6, 28.8, 27.5, 27.0, 22.6, 19.0, 19.1, 18.1, 17.0, 16.7, 14.0, 13.6, 12.3, 10.6 ppm; UV/Vis (CH<sub>2</sub>Cl<sub>2</sub>):  $\lambda_{\max}$  ( $\epsilon$ ) = 676 nm ( $3.2 \times 10^4 \text{ M}^{-1} \text{ cm}^{-1}$ ); MS (EI):  $m/z$ : 824 [M]<sup>+</sup>; HRMS: calcd for C<sub>40</sub>H<sub>47</sub>N<sub>5</sub>NiO<sub>4</sub>: 823.3244; found: 823.9922.

**Ni<sup>II</sup> 20-(3-formylphenyl)mesopurpurin-18-N-hexylimide methyl ester (19):** Compound **19** was prepared by following the experimental procedure for compound **11**. Yield: 15.3 mg (58%). <sup>1</sup>H NMR (400 MHz, CDCl<sub>3</sub>, mixture of both topoisomers):  $\delta$  = 10.36, 9.94 (s, d,  $J$  = 7.2 Hz, 1H; CHO), 9.00 (s, 1H; *meso*-H), 8.80, 8.56 (s, d,  $J$  = 7.6 Hz, 1H; Ph-H), 8.68 (s, 1H; *meso*-H), 8.08 (d,  $J$  = 6.8 Hz, 1H; Ph-H), 7.95, 7.53 (t, t,  $J$  = 8.0, 8.0 Hz, 1H; Ph-H), 7.28, 7.06 (s, d,  $J$  = 6.8 Hz, 1H; Ph-H), 4.50 (m, 1H; 17-H), 4.24 (m, 2H; N-CH<sub>2</sub>-Hexyl), 4.09 (m, 1H; 18-H), 3.68 (s, 3H; CO<sub>2</sub>Me), 3.49 (s, 3H; ring-CH<sub>3</sub>), 3.46–3.41 (m, 2H; 8-CH<sub>2</sub>CH<sub>3</sub>), 3.39–3.30 (m, 2H; 3-CH<sub>2</sub>CH<sub>3</sub>), 2.98 (s, 3H; ring-CH<sub>3</sub>), 2.71–2.66 (m, 2H; 17<sup>2</sup>-CH<sub>2</sub>), 2.32 (m, 1H; 17<sup>1</sup>-CHH), 2.19 (m, 1H; 17<sup>1</sup>-CHH), 1.88 (s, 3H; ring-CH<sub>3</sub>), 1.82 (m, 2H; CH<sub>2</sub>-Hexyl), 1.53 (m, 2H; CH<sub>2</sub>-Hexyl), 1.52 (t,  $J$  = 7.6 Hz, 3H; 8-CH<sub>2</sub>CH<sub>3</sub>), 1.44 (t,  $J$  = 7.6 Hz, 3H; 3-CH<sub>2</sub>CH<sub>3</sub>), 1.38–1.33 (m, 4H; 2

CH<sub>2</sub>-Hexyl), 0.90 (t, *J* = 7.2 Hz, 3H; CH<sub>3</sub>-Hexyl), 0.67 ppm (d, *J* = 6.8 Hz, 3H; 18-CH<sub>3</sub>); <sup>13</sup>C NMR (100 MHz, CDCl<sub>3</sub>, mixture of both topoisomers): δ = 192.4, 191.8, 174.0, 166.7, 162.8, 149.3, 148.1, 146.0, 143.7, 140.9, 138.9, 138.1, 137.7, 136.4, 134.2, 133.8, 133.5, 129.0, 128.8, 121.1, 127.8, 114.6, 110.2, 108.2, 103.8, 53.9, 53.7, 52.8, 51.6, 45.0, 39.8, 32.5, 31.6, 29.6, 28.8, 27.3, 27.0, 22.6, 19.0, 18.1, 17.0, 16.7, 14.0, 13.9, 12.3, 10.6 ppm; UV/Vis (CH<sub>2</sub>Cl<sub>2</sub>): λ<sub>max</sub> (ε) = 675 nm (3.2 × 10<sup>4</sup> M<sup>-1</sup> cm<sup>-1</sup>); MS (EI): *m/z*: 824 [M]<sup>+</sup>; HRMS: calcd for C<sub>40</sub>H<sub>47</sub>N<sub>5</sub>NiO<sub>4</sub>: 823.3244; found: 823.1112.

**Ni<sup>II</sup> 20-(*N*-Boc-4-aminomethylphenyl)mesopurpurin-18-*N*-hexylimide methyl ester (20):** Compound 20 was prepared by following the experimental procedure for compound 11. Yield: 20.1 mg (68%). <sup>1</sup>H NMR (400 MHz, CDCl<sub>3</sub>): δ = 8.97 (s, 1H; *meso*-H), 8.63 (s, 1H; *meso*-H), 8.16 (d, *J* = 8.2 Hz, 1H; Ar-H), 7.60 (d, *J* = 9.6 Hz, 1H; Ar-H), 7.22 (d, *J* = 8.8 Hz, 1H; Ar-H), 6.88 (d, *J* = 8.8 Hz, 1H; Ar-H), 5.31 (brs, 1H; NH), 4.47 (m, 3H; 17-H, Benzyl-CH<sub>2</sub>), 4.22–4.29 (m, 3H; 18-H, N-CH<sub>2</sub>-Hexyl), 3.64 (s, 3H; CO<sub>2</sub>Me), 3.46 (s, 3H; ring-CH<sub>3</sub>), 3.26–3.44 (m, 4H; 8-CH<sub>2</sub>CH<sub>3</sub>, 3-CH<sub>2</sub>CH<sub>3</sub>), 2.96 (s, 3H; ring-CH<sub>3</sub>), 2.61–2.68 (m, 2H; 17<sup>2</sup>-CH<sub>2</sub>), 2.26–2.31 (m, 1H; 17<sup>1</sup>-CHH), 2.10–2.17 (m, 1H; 17<sup>1</sup>-CHH), 1.87 (s, 3H; ring-CH<sub>3</sub>), 1.81 (m, 2H; -CH<sub>2</sub>-Hexyl), 1.35–1.44 (m, 21H; 8-CH<sub>2</sub>CH<sub>3</sub>, 3 CH<sub>2</sub>-Hexyl, 3-CH<sub>2</sub>CH<sub>3</sub>, *t*-Butyl-Me<sub>3</sub>), 0.88 (t, *J* = 6.8 Hz, 3H; CH<sub>3</sub>-Hexyl), 0.65 ppm (d, *J* = 6.4 Hz, 3H; 18-CH<sub>3</sub>); <sup>13</sup>C NMR (100 MHz, CDCl<sub>3</sub>): δ = 190, 173.8, 166.2, 163.0, 162.3, 161.7, 152.6, 150.1, 148.5, 147.7, 143.3, 141.9, 138.4, 137.9, 135.1, 134.4, 133.0, 132.9, 132.2, 120.4, 117.9, 117.7, 115.9, 114.6, 113.1, 111.8, 105.0, 101.0, 99.8, 53.0, 51.6, 50.5, 45.7, 40.1, 32.3, 31.8, 31.6, 29.6, 29.3, 28.7, 28.3, 27.8, 26.9, 22.6, 19.0, 18.2, 16.7, 16.3, 14.0, 13.8, 10.5 ppm; UV/Vis (CHCl<sub>3</sub>): λ<sub>max</sub> (ε) = 673 nm (3.1 × 10<sup>4</sup> M<sup>-1</sup> cm<sup>-1</sup>); MS (EI): *m/z*: 925 [M+H]<sup>+</sup>; HRMS: calcd for C<sub>52</sub>H<sub>62</sub>N<sub>6</sub>NiO<sub>6</sub>+H: 925.4157; found: 925.4136.

**Ni<sup>II</sup> 20-(4-hydroxyphenyl)mesopurpurin-18-*N*-hexylimide methyl ester (21):** Compound 21 was prepared by following the experimental procedure for compound 11. Yield: 15.8 mg (61%). <sup>1</sup>H NMR (400 MHz, CDCl<sub>3</sub>): δ = 8.98 (s, 1H; *meso*-H), 8.64 (s, 1H; *meso*-H), 8.05 (d, *J* = 8.2 Hz, 1H; Ar-H), 7.19 (d, *J* = 9.6 Hz, 1H; Ar-H), 6.80 (d, *J* = 8.8 Hz, 1H; Ar-H), 6.58 (d, *J* = 8.8 Hz, 1H; Ar-H), 5.44 (brs, 1H; OH), 4.49 (dd, *J* = 4.0, 9.2 Hz, 1H; 17-H), 4.14–4.29 (m, 3H; 18-H, N-CH<sub>2</sub>-Hexyl), 3.66 (s, 3H; CO<sub>2</sub>Me), 3.48 (s, 3H; ring-CH<sub>3</sub>), 3.26–3.45 (m, 4H; 8-CH<sub>2</sub>CH<sub>3</sub>, 3-CH<sub>2</sub>CH<sub>3</sub>), 2.97 (s, 3H; ring-CH<sub>3</sub>), 2.62–2.71 (m, 2H; 17<sup>2</sup>-CH<sub>2</sub>), 2.28–2.34 (m, 1H; 17<sup>1</sup>-CHH), 2.04–2.17 (m, 1H; 17<sup>1</sup>-CHH), 1.96 (s, 3H; ring-CH<sub>3</sub>), 1.83 (m, 2H; CH<sub>2</sub>-Hexyl), 1.38–1.49 (m, 12H; 8-CH<sub>2</sub>CH<sub>3</sub>, 3 CH<sub>2</sub>-Hexyl, 3-CH<sub>2</sub>CH<sub>3</sub>), 0.89 (t, *J* = 6.8 Hz, 3H; CH<sub>3</sub>-Hexyl), 0.69 ppm (d, *J* = 6.4 Hz, 3H; 18-CH<sub>3</sub>); <sup>13</sup>C NMR (100 MHz, CDCl<sub>3</sub>): δ = 174.0, 166.7, 162.9, 161.2, 158.4, 155.3, 149.0, 145.4, 143.6, 143.1, 140.8, 139.2, 138.6, 135.7, 135.3, 133.3, 133.0, 132.0, 127.8, 120.2, 114.7, 111.3, 108.3, 105.0, 103.1, 97.2, 83.5, 53.6, 51.6, 45.0, 39.8, 32.5, 31.6, 28.8, 27.6, 27.0, 24.8, 22.6, 19.0, 18.2, 17.0, 16.7, 14.0, 13.6, 12.3, 10.6 ppm; UV/Vis: λ<sub>max</sub> (ε) = 671 nm (3.6 × 10<sup>4</sup> M<sup>-1</sup> cm<sup>-1</sup>); MS (EI): *m/z*: 812 [M+H]<sup>+</sup>; HRMS: calcd for C<sub>46</sub>H<sub>51</sub>N<sub>5</sub>NiO<sub>5</sub>+H: 812.3316; found: 812.3313.

**Ni<sup>II</sup> 20-(4-hydroxymethylphenyl)mesopurpurin-18-*N*-hexylimide methyl ester (22):** Compound 22 was prepared by following the experimental procedure for compound 11. Yield: 12.6 mg (48%). <sup>1</sup>H NMR (400 MHz, CDCl<sub>3</sub>): δ = 9.06 (s, 1H; *meso*-H), 8.68 (s, 1H; *meso*-H), 8.22 (d, *J* = 8.2 Hz, 1H; Ar-H), 7.84 (d, *J* = 9.6 Hz, 1H; Ar-H), 7.38 (d, *J* = 8.8 Hz, 1H; Ar-H), 6.78 (d, *J* = 8.8 Hz, 1H; Ar-H), 4.90 (s, 2H; Benzyl-CH<sub>2</sub>), 4.50 (dd, *J* = 4.0, 9.2 Hz, 1H; 17-H), 4.14–4.31 (m, 3H; 18-H, N-CH<sub>2</sub>-Hexyl), 3.65 (s, 3H; CO<sub>2</sub>Me), 3.51 (s, 3H; ring-CH<sub>3</sub>), 3.24–3.50 (m, 4H; 8-CH<sub>2</sub>CH<sub>3</sub>, 3-CH<sub>2</sub>CH<sub>3</sub>), 2.99 (s, 3H; ring-CH<sub>3</sub>), 2.60–2.74 (m, 2H; 17<sup>2</sup>-CH<sub>2</sub>), 2.30–2.38 (m, 1H; 17<sup>1</sup>-CHH), 2.10–2.20 (m, 1H; 17<sup>1</sup>-CHH), 1.98 (s, 3H; ring-CH<sub>3</sub>), 1.80–1.94 (m, 2H; CH<sub>2</sub>-Hexyl), 1.32–1.60 (m, 12H; 8-CH<sub>2</sub>CH<sub>3</sub>, 3 CH<sub>2</sub>-Hexyl, 3-CH<sub>2</sub>CH<sub>3</sub>), 0.96 (t, *J* = 6.8 Hz, 3H; CH<sub>3</sub>-Hexyl), 0.64 ppm (d, *J* = 6.4 Hz, 3H; 18-CH<sub>3</sub>); <sup>13</sup>C NMR (100 MHz, CDCl<sub>3</sub>): δ = 173.9, 166.7, 161.2, 157.8, 149.0, 148.6, 145.5, 143.6, 143.1, 140.8, 140.5, 139.1, 139.0, 138.7, 135.8, 135.0, 133.3, 132.5, 132.0, 126.6, 120.3, 115.2, 111.5, 108.3, 103.3, 97.2, 65.0, 53.6, 51.5, 45.0, 39.8, 32.5, 31.6, 29.6, 28.8, 27.5, 27.0, 22.6, 19.0, 18.2, 17.0, 16.7, 14.0, 13.5, 12.3, 10.6 ppm; UV/Vis (CHCl<sub>3</sub>): λ<sub>max</sub> (ε) = 671 nm (3.3 × 10<sup>4</sup> M<sup>-1</sup> cm<sup>-1</sup>); MS (EI): *m/z*: 826 [M+H]<sup>+</sup>; HRMS: calcd for C<sub>47</sub>H<sub>53</sub>N<sub>5</sub>NiO<sub>5</sub>+H: 826.3473; found: 826.3482.

**Ni<sup>II</sup> 20-(4-isopropylthiophenyl)mesopurpurin-18-*N*-hexylimide methyl ester (23):** Compound 23 was prepared by following the experimental

procedure for compound 11. Yield: 18.3 mg (66%). <sup>1</sup>H NMR (400 MHz, CDCl<sub>3</sub>): δ = 8.98 (s, 1H; *meso*-H), 8.65 (s, 1H; *meso*-H), 8.15 (d, *J* = 8.2 Hz, 1H; Ar-H), 7.73 (d, *J* = 9.6 Hz, 1H; Ar-H), 7.34 (d, *J* = 8.8 Hz, 1H; Ar-H), 6.66 (d, *J* = 8.8 Hz, 1H; Ar-H), 4.50 (dd, *J* = 4.0, 9.2 Hz, 1H; 17-H), 4.16–4.24 (m, 3H; 18-H, N-CH<sub>2</sub>-Hexyl), 3.66 (s, 3H; CO<sub>2</sub>Me), 3.49 (s, 3H; ring-CH<sub>3</sub>), 3.30–3.55 (m, 4H; 8-CH<sub>2</sub>CH<sub>3</sub>, 3-CH<sub>2</sub>CH<sub>3</sub>), 2.98 (s, 3H; ring-CH<sub>3</sub>), 2.63–2.70 (m, 2H; 17<sup>2</sup>-CH<sub>2</sub>), 2.28–2.36 (m, 1H; 17<sup>1</sup>-CHH), 2.10–2.17 (m, 1H; 17<sup>1</sup>-CHH), 1.95 (s, 3H; ring-CH<sub>3</sub>), 1.81–1.85 (m, 2H; CH<sub>2</sub>-Hexyl), 1.37–1.53 (m, 19H; 8-CH<sub>2</sub>CH<sub>3</sub>, (CH<sub>3</sub>)<sub>2</sub>H-S, (CH<sub>3</sub>)<sub>2</sub>H-S, 3 CH<sub>2</sub>-Hexyl, 3-CH<sub>2</sub>CH<sub>3</sub>), 0.96 (t, *J* = 6.8 Hz, 3H; CH<sub>3</sub>-Hexyl), 0.69 ppm (d, *J* = 6.4 Hz, 3H; 18-CH<sub>3</sub>); <sup>13</sup>C NMR (100 MHz, CDCl<sub>3</sub>): δ = 174.0, 166.7, 162.9, 161.2, 157.7, 149.6, 148.5, 145.6, 143.6, 143.1, 140.9, 139.0, 138.7, 137.9, 135.8, 135.6, 134.9, 133.4, 132.9, 132.2, 131.1, 130.9, 120.4, 111.1, 108.3, 103.3, 97.3, 53.6, 51.6, 45.0, 39.8, 38.0, 32.2, 31.7, 28.8, 27.6, 27.0, 22.7, 19.0, 18.8, 17.9, 17.0, 16.8, 15.2, 14.0, 12.2, 10.5 ppm; UV/Vis (CHCl<sub>3</sub>): λ<sub>max</sub> (ε) = 672 nm (3.2 × 10<sup>4</sup> M<sup>-1</sup> cm<sup>-1</sup>); MS (EI): *m/z*: 870 [M]<sup>+</sup>; HRMS: calcd for C<sub>49</sub>H<sub>57</sub>N<sub>5</sub>NiO<sub>5</sub>+H: 870.3557; found: 870.3492.

**Ni<sup>II</sup> 20-(4-aminomethylphenyl)mesopurpurin-18-*N*-hexylimide methyl ester (26a):** Compound 20 (20 mg, 0.021 mmol) was treated with TFA/CH<sub>2</sub>Cl<sub>2</sub> (9:1, 5 mL) in an inert atmosphere for 6 h. The reaction mixture was concentrated under vacuum and the resulting crude product was purified through a column of silica gel to provide pure 26a. Yield: 11.7 mg (66%). <sup>1</sup>H NMR (400 MHz, CDCl<sub>3</sub>): δ = 8.41 (s, 1H; *meso*-H), 8.40 (s, 1H; *meso*-H), 8.37 (d, *J* = 8.2 Hz, 1H; Ar-H), 7.87 (d, *J* = 9.6 Hz, 1H; Ar-H), 7.43 (d, *J* = 8.8 Hz, 1H; Ar-H), 6.87 (d, *J* = 8.8 Hz, 1H; Ar-H), 4.28 (m, 3H; 17-H, Benzyl-CH<sub>2</sub>), 4.08 (q, *J* = 6.8 Hz, 1H; 18-H), 3.98 (s, 2H; NH<sub>2</sub>), 4.22–4.29 (m, 2H; N-CH<sub>2</sub>-Hexyl), 3.67 (s, 3H; CO<sub>2</sub>Me), 3.11–3.30 (m, 2H; 8-CH<sub>2</sub>CH<sub>3</sub>), 2.86–3.00 (m, 5H; 3-CH<sub>2</sub>CH<sub>3</sub>, ring-CH<sub>3</sub>), 2.83 (s, 3H; ring-CH<sub>3</sub>), 2.56 (t, *J* = 8.0 Hz, 2H; 17<sup>2</sup>-CH<sub>2</sub>), 2.04–2.16 (m, 2H; 17<sup>1</sup>-CHH, 17<sup>1</sup>-CHH), 1.88 (s, 3H; ring-CH<sub>3</sub>), 1.61 (m, 2H; CH<sub>2</sub>-Hexyl), 1.27–1.55 (m, 9H; 8-CH<sub>2</sub>CH<sub>3</sub>, 3 CH<sub>2</sub>-Hexyl), 1.20 (t, *J* = 7.6 Hz, 3H; 3-CH<sub>2</sub>CH<sub>3</sub>), 0.88 (t, *J* = 6.8 Hz, 3H; CH<sub>3</sub>-Hexyl), 0.59 ppm (d, *J* = 6.4 Hz, 3H; 18-CH<sub>3</sub>); <sup>13</sup>C NMR (100 MHz, CDCl<sub>3</sub>): δ = 175.5, 174.2, 167.5, 163.3, 154.0, 150.5, 145.2, 145.0, 142.1, 140.8, 139.5, 137.1, 136.4, 134.3, 133.9, 132.6, 132.4, 131.3, 127.5, 127.0, 116.2, 112.3, 106.5, 102.1, 97.7, 55.6, 51.5, 47.1, 40.4, 32.8, 31.7, 30.0, 29.6, 29.3, 28.9, 27.1, 22.7, 22.6, 20.7, 19.3, 19.1, 17.4, 16.7, 14.0, 13.2, 12.4, 11.0 ppm; UV/Vis (CHCl<sub>3</sub>): λ<sub>max</sub> (ε) = 672 nm (3.1 × 10<sup>4</sup> M<sup>-1</sup> cm<sup>-1</sup>); MS (EI): *m/z*: 825 [M+H]<sup>+</sup>; HRMS: calcd for C<sub>47</sub>H<sub>54</sub>N<sub>6</sub>NiO<sub>4</sub>+H: 825.3633; found: 825.3649.

**20-(4-aminomethylphenyl) mesopurpurin-18-*N*-hexylimide methyl ester (26b):** Compound 26b was prepared by treating compound 26a (25 mg, 0.030 mmol) with conc. H<sub>2</sub>SO<sub>4</sub> (4 mL) in an ice-cold bath and stirring at room temperature for 30 min. The crude mixture was poured into ice-cold water (25 mL) and extracted with dichloromethane (2 × 50 mL). The resulting organic layer was washed with a sat. bicarbonate solution and then water. The crude product was obtained by evaporating the organic layer, which was purified by silica gel column chromatography. Yield: 9.7 mg (42%). <sup>1</sup>H NMR (400 MHz, CDCl<sub>3</sub>): δ = 9.56 (s, 1H; *meso*-H), 9.28 (s, 1H; *meso*-H), 8.13 (d, *J* = 8.2 Hz, 1H; Ar-H), 7.68 (d, *J* = 9.6 Hz, 1H; Ar-H), 7.45 (d, *J* = 8.8 Hz, 1H; Ar-H), 7.33 (d, *J* = 8.8 Hz, 1H; Ar-H), 5.16 (m, 1H; 17-H), 4.39–4.44 (m, 2H; N-CH<sub>2</sub>-Hexyl), 4.22 (q, *J* = 7.2 Hz, 1H; 18-H), 4.04 (brs, 2H; NH<sub>2</sub>), 3.81 (s, 2H; Benzyl-CH<sub>2</sub>), 3.61–3.67 (m, 4H; 8-CH<sub>2</sub>CH<sub>3</sub>, 3-CH<sub>2</sub>CH<sub>3</sub>), 3.56 (s, 3H; CO<sub>2</sub>Me), 3.18 (s, 3H; ring-CH<sub>3</sub>), 2.69–2.76 (m, 1H; 17<sup>1</sup>-CHH), 2.25–2.45 (m, 3H; 17<sup>2</sup>-CH<sub>2</sub>, 17<sup>1</sup>-CHH), 2.16 (s, 3H; ring-CH<sub>3</sub>), 2.13 (s, 3H; ring-CH<sub>3</sub>), 1.93–2.09 (m, 4H; 2 CH<sub>2</sub>-Hexyl), 1.66 (t, *J* = 7.1 Hz, 3H; 3-CH<sub>2</sub>CH<sub>3</sub>), 1.54–1.58 (m, 5H; 8-CH<sub>2</sub>CH<sub>3</sub>, CH<sub>2</sub>-Hexyl), 1.24–1.49 (m, 2H; CH<sub>2</sub>-Hexyl), 0.85–0.94 (m, 6H; CH<sub>3</sub>-Hexyl, 18-CH<sub>3</sub>), 0.31 (brs, 1H), -0.33 ppm (brs, 1H); <sup>13</sup>C NMR (100 MHz, CDCl<sub>3</sub>): δ = 172.2, 166.7, 162.9, 157.8, 156.0, 150.5, 145.2, 145.0, 142.1, 140.8, 139.5, 137.1, 136.4, 134.3, 133.9, 132.6, 132.4, 131.3, 127.5, 127.0, 116.2, 112.3, 106.5, 104.2, 102.1, 97.7, 53.6, 51.5, 45.1, 39.8, 32.5, 31.7, 29.6, 28.8, 27.1, 22.7, 22.6, 20.7, 19.3, 19.1, 17.4, 16.7, 14.0, 13.2, 12.3, 10.6 ppm; UV/Vis (CH<sub>2</sub>Cl<sub>2</sub>): λ<sub>max</sub> (ε) = 705 nm (5.1 × 10<sup>4</sup> M<sup>-1</sup> cm<sup>-1</sup>); MS (EI): *m/z*: 769 [M+H]<sup>+</sup>; HRMS: calcd for C<sub>47</sub>H<sub>56</sub>N<sub>6</sub>O<sub>4</sub>+H: 769.4436; found: 769.4451.

**Ni<sup>II</sup> purpurinimide-cyanine dye conjugate 27:** Ni<sup>II</sup> 20-(4-aminomethylphenyl)mesopurpurin-18-*N*-hexylimide methyl ester (26a; 20 mg, 0.1 equiv) was placed in a dry round-bottomed flask (50.0 mL)

and dissolved in anhydr. DMF (10 mL). Cyanine dye **25** (0.12 equiv), *N*-ethyl-*N'*-(3-dimethylaminopropyl)carbodiimide hydrochloride (0.15 equiv), and 4-dimethylaminopyridine (DMAP; 0.11 equiv) were added and the resultant mixture was stirred for 12 h at room temperature under N<sub>2</sub>. The reaction mixture was evaporated under vacuum and then the crude product obtained was purified through a column of silica gel by using 5–20% methanol/dichloromethane as eluent to yield 35% (14.8 mg) of the desired conjugate. <sup>1</sup>H NMR (400 MHz, 20% CD<sub>3</sub>OD/5% [D<sub>6</sub>]DMSO/CDCl<sub>3</sub>): δ = 8.84 (s, 1H; *meso*-H), 8.68 (d, *J* = 14 Hz, 2H), 8.58 (s, 1H; *meso*-H), 7.95–7.99 (m, 3H), 7.87 (d, *J* = 9.6 Hz, 2H), 7.55–7.59 (m, 3H), 7.46 (d, *J* = 8.8 Hz, 2H), 7.33–7.38 (6H), 7.01–7.05 (m, 3H), 6.30 (d, *J* = 8.2 Hz, 2H), 6.05 (d, *J* = 8.4 Hz, 2H), 4.60 (s, 2H; Benzyl-CH<sub>2</sub>), 4.06–4.21 (m, 7H), 3.91 (q, *J* = 7.1 Hz, 1H), 3.51 (s, 3H; CO<sub>2</sub>Me), 3.32 (m, 8H), 2.81–2.84 (m, 12H), 2.61 (d, *J* = 6.4 Hz, 3H), 2.44 (t, *J* = 8.0 Hz, 3H), 2.15 (s, 3H), 2.13 (s, 3H), 2.04–2.16 (m, 2H), 1.86 (m, 12H), 1.73 (m, 2H), 1.64 (s, 3H), 1.42–1.58 (m, 10H), 0.89 (m, 6H), 0.26 ppm (d, *J* = 6.4 Hz, 3H; 18-CH<sub>3</sub>); <sup>13</sup>C NMR (150 MHz, 20% CD<sub>3</sub>OD/5% [D<sub>6</sub>]DMSO/CDCl<sub>3</sub>): δ = 174.8, 174.3, 168.0, 167.3, 163.9, 161.9, 158.3, 149.8, 149.6, 145.8, 145.4, 144.4, 143.3, 142.2, 139.9, 139.75, 139.70, 139.4, 138.9, 138.7, 136.1, 135.7, 134.2, 134.1, 134.0, 132.8, 132.4, 132.2, 131.6, 131.2, 130.4, 128.8, 128.5, 128.0, 127.5, 127.2, 126.3, 125.6, 122.4, 120.3, 112.0, 110.9, 109.1, 103.8, 101.2, 54.1, 51.9, 51.4, 50.8, 45.4, 44.7, 43.5, 40.2, 32.8, 32.0, 29.1, 27.8, 27.6, 27.3, 26.8, 26.7, 23.0, 22.8, 21.1, 19.3, 19.2, 18.3, 17.2, 16.8, 14.1, 13.6, 12.4, 10.7 ppm; UV/Vis (MeOH): λ<sub>max</sub> (ε) = 677 (3.2 × 10<sup>4</sup>), 835 nm (19.2 × 10<sup>4</sup> m<sup>-1</sup> cm<sup>-1</sup>); MS (EI): *m/z*: 1751 [M–H]<sup>+</sup>; HRMS: calcd for C<sub>100</sub>H<sub>108</sub>N<sub>8</sub>NiO<sub>11</sub>S<sub>3</sub>: 1750.6653; found: 1750.6611.

**Purpurinimide–cyanine dye conjugate 28:** Compound **28** was prepared by following the experimental procedure for compound **27**. Yield: 13.6 mg (31%). <sup>1</sup>H NMR (400 MHz, 20% CD<sub>3</sub>OD/CDCl<sub>3</sub>): δ = 8.80 (s, 1H; *meso*-H), 8.68 (s, 1H; *meso*-H), 8.52 (d, *J* = 14 Hz, 2H), 7.95–7.99 (m, 3H), 7.87 (d, *J* = 9.6 Hz, 2H), 7.55–7.59 (m, 3H), 7.46 (d, *J* = 8.8 Hz, 2H), 7.33–7.38 (6H), 7.01–7.05 (m, 3H), 6.30 (d, *J* = 8.2 Hz, 2H), 6.05 (d, *J* = 8.4 Hz, 2H), 4.60 (s, 2H; Benzyl-CH<sub>2</sub>), 4.06–4.21 (m, 7H), 3.91 (q, *J* = 7.1 Hz, 1H), 3.51 (s, 3H; CO<sub>2</sub>Me), 3.32 (m, 8H), 2.81–2.84 (m, 12H), 2.61 (d, *J* = 7.0 Hz, 3H), 2.44 (t, *J* = 8.0 Hz, 3H), 2.15 (s, 3H), 2.13 (s, 3H), 2.04–2.16 (m, 2H), 1.86 (m, 12H), 1.73 (m, 2H), 1.64 (s, 3H), 1.42–1.58 (m, 14H), 0.89 (m, 6H), 0.26 (d, *J* = 6.4 Hz, 3H; 18-CH<sub>3</sub>), 0.22 (brs, 1H; NH), –0.20 ppm (brs, 1H; NH) ppm; UV/Vis (MeOH): λ<sub>max</sub> (ε) = 705 (5.1 × 10<sup>4</sup>), 835 nm (19.3 × 10<sup>4</sup> m<sup>-1</sup> cm<sup>-1</sup>); MS (EI): *m/z*: 1694 [M–H]<sup>+</sup>; HRMS: calcd for C<sub>100</sub>H<sub>110</sub>N<sub>8</sub>O<sub>11</sub>S<sub>3</sub>: 1694.7456; found: 1694.7511.

**Ni<sup>II</sup> 20-(4-maleimidophenyl)mesopurpurin-18-*N*-hexylimide methyl ester (30):** The aminophenylpurpurin **14** (25 mg, 0.030 mmol) was heated at reflux with maleic anhydride (15 mg, 0.15 mmol) in acetic anhydride (5 mL) and stirred at room temperature for 12 h. The resulting mixture was treated with NaOAc in AcOH and then heated at reflux for 3 h. The resulting crude product was diluted with dichloromethane and the mixture was neutralized with a sat. bicarbonate solution. The organic layer was concentrated and the crude obtained was purified on a silica gel column by elution with 30% EtOAc/hexane as eluent to obtain the desired maleimide derivative **30**. Yield: 12.8 mg (48%). <sup>1</sup>H NMR (400 MHz, CDCl<sub>3</sub>): δ = 8.97 (s, 1H; *meso*-H), 8.65 (s, 1H; *meso*-H), 8.32 (d, *J* = 8.2 Hz, 1H; Ar-H), 7.76 (d, *J* = 9.6 Hz, 1H; Ar-H), 7.36 (d, *J* = 8.8 Hz, 1H; Ar-H), 6.91 (s, 2H; CO–CH=CH–CO), 6.82 (d, *J* = 8.8 Hz, 1H; Ar-H), 4.50 (m, 1H; 17-H), 4.16–4.25 (m, 3H; N–CH<sub>2</sub>–Hexyl, 18-H), 3.65 (s, 3H; CO<sub>2</sub>Me), 3.48 (s, 3H; ring-CH<sub>3</sub>), 3.27–3.50 (m, 4H; 8-CH<sub>2</sub>CH<sub>3</sub>, 3-CH<sub>2</sub>CH<sub>3</sub>), 2.96 (s, 3H; ring-CH<sub>3</sub>), 2.67 (t, *J* = 8.0 Hz, 2H; 17<sup>2</sup>-CH<sub>2</sub>), 2.26–2.36 (m, 2H; 17<sup>1</sup>-CHH, 17<sup>1</sup>-CHH), 1.93 (s, 3H; ring-CH<sub>3</sub>), 1.77–1.85 (m, 2H; CH<sub>2</sub>-Hexyl), 1.23–1.53 (m, 10H; 8-CH<sub>2</sub>CH<sub>3</sub>, 3-CH<sub>2</sub>CH<sub>3</sub>, 2 CH<sub>2</sub>-Hexyl), 0.82–0.92 (m, 5H; CH<sub>3</sub>-Hexyl, CH<sub>2</sub>-Hexyl), 0.69 ppm (d, *J* = 6.4 Hz, 3H; 18-CH<sub>3</sub>); <sup>13</sup>C NMR (100 MHz, CDCl<sub>3</sub>): δ = 174.0, 172.0, 166.7, 162.8, 161.3, 157.4, 149.2, 145.8, 143.6, 143.0, 140.3, 139.0, 135.9, 134.7, 134.2, 133.5, 133.1, 132.5, 130.9, 127.9, 126.3, 120.5, 110.5, 108.4, 103.6, 97.3, 67.7, 53.8, 51.6, 45.0, 39.8, 35.8, 32.5, 31.6, 29.6, 28.8, 27.6, 27.0, 22.6, 20.5, 19.0, 18.2, 17.0, 16.7, 14.0, 13.6, 12.3, 10.6 ppm; UV/Vis (CH<sub>2</sub>Cl<sub>2</sub>): λ<sub>max</sub> (ε) = 671 nm (3.8 × 10<sup>4</sup> m<sup>-1</sup> cm<sup>-1</sup>); MS (EI): *m/z*: 891 [M+H]<sup>+</sup>; HRMS: calcd for C<sub>50</sub>H<sub>52</sub>N<sub>6</sub>NiO<sub>6</sub>+H: 891.3375; found: 891.3369.

**Photostability measurements:** In brief, conjugates **27** and **28** were formulated in 1% Tween 80 in D5W and then diluted in 17% bovine calf serum (BCS) to 5 μm. Changes in the concentration of the cyanine dye portion of the conjugates were measured by a spectrophotometer at user-specified intervals post-irradiation. The solutions were placed individually in fluorescent cuvettes and exposed to radiation at 705 nm (**28**) and 677 nm (**27**) while being magnetically stirred to ensure the homogeneous distribution of singlet oxygen. An argon-pumped dye laser was used with a power output of 530 mW for a 3 cm spot size. This yields 75 mW cm<sup>-2</sup> at the center plane of the cuvette. The decrease in the absorbance spectra during irradiation was predominantly attributed to photodegradation (photobleaching).

**In vitro PDT efficacy:** The photosensitizing activities of the drugs **27** and **28** were determined in the Colon 26 tumor cell line as previously described.<sup>[46]</sup> The Colon 26 tumor cells were grown in RPMI 1640 medium with 10% fetal calf serum, 1% L-glutamine, 1% penicillin, and 1% streptomycin. Cells were maintained in 5% CO<sub>2</sub>/95% air and 100% humidity. To determine the PDT efficacy, these cells were placed in 96-well plates at a density of 5 × 10<sup>3</sup> cells per well in complete media. After overnight incubation at 37 °C, the photosensitizers were added at variable concentrations (from 0.0193 to 6 μm) and incubated at 37 °C for 24 h in the dark. Prior to light treatment, the cells were replaced with drug-free complete media. The cells were then illuminated with an argon-pumped dye laser set at 706 nm for drug **27** and at 680 nm for drug **28** at a dose rate of 3.2 mW cm<sup>-2</sup> with variable light doses (0–2 J cm<sup>-2</sup>). After PDT, the cells were incubated for 48 h at 37 °C in the dark. Following incubation, a 4.0 mg mL<sup>-1</sup> solution of 3-(4,5-dimethylthiazol-2-yl)-2,5-diphenyltetrazolium bromide (MTT; 10 μL) dissolved in PBS (Sigma, St. Louis, MO) was added to each well. After 4 h of further incubation at 37 °C, the MTT and media were removed and DMSO (100 μL; Sigma, St. Louis, MO) was added to solubilize the formazine crystals. The 96-well plate was then analyzed with a microtiter plate reader (BioTek Instruments, Inc., ELx800 Absorbance Microplate Reader) at an absorbance of 570 nm. The results were plotted as percent survival of the corresponding dark (drug, no light) control for each compound tested (see Figure 10). Each data point represents the mean of three separate experiments, and the error bars are the standard deviation. Each experiment was performed with six replicate wells.

**Optical imaging setup:** Fluorescence planar optical imaging was performed in accordance with the Guide for the Use of Laboratory Animals. The mice (three per group) bearing subcutaneous Colon-26 tumors on the shoulder were anesthetized with ketamine/xylazine by intraperitoneal injection. The conjugates **27** and **28** and compound **25** were injected intravenously at 0.3 μmol kg<sup>-1</sup> and then imaged 24, 48, and 72 h post-injection.

Whole-body fluorescence imaging was carried out with a 12 Bit monochrome Nuance CCD Camera (CRI, Woburn, MA). A 782 nm BWF light source (B&W-Tek, Newark, DE), continuous wave laser was used to excite the cyanine dye (CD) and the fluorescence emission was collected beyond 830 nm with an 800 and 830 nm long-pass filter in series. To superimpose the white-light image of the mouse on the fluorescence image of compound **25**, an image of the mouse with a tungsten halogen white-light source was first taken, followed by an image as described above for the CD. The white light and fluorescence images were superimposed by using the NIH ImageJ software. The fluorescence images for **25**, **27**, and **28** were normalized to the same lookup table (LUT) and minimum and maximum brightness in ImageJ.

**Electrochemical measurements:** Cyclic voltammetry was carried out with an EG&G Model 173 potentiostat/galvanostat. A home-made three-electrode cell was used and consisted of a platinum button or glassy carbon working electrode, a platinum wire counter electrode, and a saturated calomel reference electrode (SCE). The SCE was separated from the bulk of the solution by a fritted-glass bridge of low porosity that contained the solvent/supporting electrolyte mixture. All potentials are referenced to the SCE.

UV/Vis spectroelectrochemical experiments were performed with an optically transparent platinum thin-layer electrode of the type described in the literature.<sup>[47]</sup> Potentials were applied with an EG&G Model 173 po-

tentiostat/galvanostat. Time-resolved UV/Vis spectra were recorded with a Hewlett-Packard Model 8453 diode-array rapid scanning spectrophotometer.

Tetra-*n*-butylammonium perchlorate (TBAP,  $\geq 99\%$ ) was purchased from Fluka Chemical Co., recrystallized from ethyl alcohol, and dried under vacuum at 40°C for at least 1 week prior to use. DMSO ( $\geq 99.9\%$ ) was obtained from Sigma–Aldrich Chemical Co. and used without further purification.

### Acknowledgements

Financial support from the NIH (R.K.P., CA55791 and CA127369), the Roswell Park Alliance Foundation (R.K.P.), the Robert A. Welch Foundation (K.M.K., Grant E-680) and the shared resources of the Roswell Park Cancer Support (Grant P30A15056) is gratefully acknowledged. Mass spectrometry analyses were performed at the Biopolymer Facility, Roswell Park Cancer Institute, Buffalo and the Michigan State University, East Lansing, Michigan.

- [1] M. Ethirajan, Y. Chen, P. Joshi, R. K. Pandey, *Chem. Soc. Rev.* **2011**, 40, 340–362.
- [2] D. Kessel, *Adv. Drug Delivery Rev.* **2004**, 56, 7.
- [3] D. E. G. J. Dolmans, D. Fukumura, R. K. Jain, *Nat. Rev. Cancer* **2003**, 3, 380–390.
- [4] N. L. Oleinick, R. L. Morris, I. Belichenko, *Photochem. Photobiol. Sci.* **2002**, 1, 1–21.
- [5] H. Ali, J. E. van Lier, *Chem. Rev.* **1999**, 99, 2379–2450.
- [6] G. H. Vicente, M. Sibrián-Vázquez in *Handbook of Porphyrin Science* (Eds. K. M. Kadish, K. M. Smith, R. Guilard), World Scientific, New Jersey, **2010**.
- [7] R. K. Pandey, L. N. Goswami, Y. Chen, A. Gryshuk, J. R. Missert, Allan Oseroff, T. J. Dougherty, *Lasers Surg. Med.* **2006**, 38, 445–468.
- [8] R. K. Pandey, A. B. Sumlin, S. Constantine, M. Aoudia, W. R. Potter, D. A. Bellnier, B. W. Henderson, M. R. Rodgers, K. M. Smith, T. J. Dougherty, *Photochem. Photobiol.* **1996**, 64, 194–204.
- [9] B. W. Henderson, D. A. Bellnier, W. R. Greco, A. Sharma, R. K. Pandey, L. Vaughan, K. R. Weishaupt, T. J. Dougherty, *Cancer Res.* **1997**, 57, 4000–4007.
- [10] T. J. Dougherty, R. K. Pandey, H. R. Nava, J. A. Smith, H. O. Douglass, S. B. Edge, D. A. Bellnier, L. O'Molloy, M. Cooper, *Proc. SPIE-Int. Soc. Opt. Eng.* **2000**, 3909, 25–27.
- [11] D. A. Bellnier, W. R. Greco, G. M. Loewen, V. Nava, A. O. Oseroff, R. K. Pandey, T. Tsuchida, T. J. Dougherty, *Cancer Res.* **2003**, 63, 1806–1813.
- [12] G. M. Loewen, R. K. Pandey, D. A. Bellnier, B. W. Henderson, T. J. Dougherty, *Lasers Surg. Med.* **2006**, 38, 364–370.
- [13] D. A. Bellnier, W. R. Greco, H. Nava, G. M. Loewen, A. R. Oseroff, T. J. Dougherty, *Cancer Chemother. Pharmacol.* **2006**, 57, 40–45.
- [14] T. M. Anderson, T. J. Dougherty, D. F. Tan, A. Sumlin, J. M. Schlosin, P. M. Kanter, *Anticancer Res.* **2003**, 23, 3713–3718.
- [15] W. Mo, D. Rohrbach, U. Sunar, *J. Biol. Inorg. Chem. J. Biomed. Optics* **2012**, 17, 071306–071308.
- [16] G. Zheng, S. Camacho, W. Potter, D. A. Bellnier, B. W. Henderson, T. J. Dougherty, R. K. Pandey, *J. Med. Chem.* **2001**, 44, 1540–1559.
- [17] A. Rungta, G. Zheng, J. R. Missert, W. Potter, T. J. Dougherty, R. K. Pandey, *Bioorg. Med. Chem. Lett.* **2000**, 10, 1463–1466.
- [18] A. L. Gryshuk, A. Graham, S. K. Pandey, W. R. Potter, J. R. Missert, A. Oseroff, T. J. Dougherty, R. K. Pandey, *Photochem. Photobiol.* **2002**, 76, 555–559.
- [19] G. Zheng, W. R. Potter, A. Sumlin, T. J. Dougherty, R. K. Pandey, *Bioorg. Med. Chem. Lett.* **2000**, 10, 123–127.
- [20] G. Zheng, A. Graham, M. Shibata, J. R. Missert, A. Oseroff, T. J. Dougherty, R. K. Pandey, *J. Org. Chem.* **2001**, 66, 8709–8716.
- [21] X. Zheng, J. Morgan, S. K. Pandey, Y. Chen, E. Tracy, H. Baumann, J. R. Missert, C. Batt, J. Jackson, D. A. Bellnier, B. W. Henderson, R. K. Pandey, *J. Med. Chem.* **2009**, 52, 4306–4318.
- [22] A. Srivatsan, M. Ethirajan, S. K. Pandey, S. Dubey, X. Zheng, T.-H. Liu, M. Shibata, J. Missert, J. Morgan, R. K. Pandey, *Mol. Pharm.* **2011**, 8, 1186–1197 and references therein.
- [23] A. Srivatsan, Y. Wang, P. Joshi, M. Sajjad, Y. Chen, C. Liu, K. Thanakpan, J. R. Missert, E. Tracy, J. Morgan, N. Rigual, H. Baumann, R. K. Pandey, *J. Med. Chem.* **2011**, 54, 6859–6873 and references therein.
- [24] M. P. A. Williams, M. Ethirajan, K. Ohkubo, P. Chen, P. Pera, J. Morgan, W. H. White, M. Shibata, S. Fukuzumi, K. M. Kadish, R. K. Pandey, *Bioconjugate Chem.* **2011**, 22, 2283–2285 and references therein.
- [25] J. A. Sperryak, W. H. White, M. Ethirajan, N. J. Patel, L. Goswami, Y. Chen, S. Turowaki, J. R. Missert, C. Batt, R. Mazurchuk, R. K. Pandey, *Bioconjugate Chem.* **2010**, 21, 828–835 and references therein.
- [26] J. Krzystek, J. Telser, L. A. Pardi, D. P. Goldberg, B. M. Hoffman, L. Brunel, *Inorg. Chem.* **1999**, 38, 6121.
- [27] G. Jori, S. B. Brown, *Photochem. Photobiol. Sci.* **2004**, 3, 403–405.
- [28] G. Jori, C. Fabris, M. Soncin, S. Ferro, C. Coppellotti, D. Dei, L. Fantetti, G. Chiti, G. Roncucci, *Lasers Surg. Med.* **2006**, 38, 468–481.
- [29] M. R. Hamblin, T. Hasan, *Photochem. Photobiol. Sci.* **2004**, 3, 436–450.
- [30] M. Ethirajan, P. Joshi, W. H. White, K. Phkubo, S. Fukuzumi, R. K. Pandey, *Org. Lett.* **2011**, 13, 1956–1959.
- [31] A. Suzuki, *J. Organomet. Chem.* **1999**, 576, 147–168.
- [32] E. Hao, F. R. Fronczek, M. G. Vicente, *Chem. Commun.* **2006**, 4900–4902.
- [33] L. Jiao, E. Hao, F. R. Fronczek, M. G. Vicente, K. M. Smith, *Chem. Commun.* **2006**, 3900–3902.
- [34] Y. M. A. Yamada, K. Takeda, H. Takashashi, S. Ikegami, *J. Org. Chem.* **2003**, 68, 7733–7741.
- [35] C. R. Fontana, A. D. Abernethy, S. Som, K. Ruggiero, S. Doucette, R. C. Marcantonio, C. I. Bousios, R. Kent, J. M. Goodson, A. C. R. Tanner, N. S. Soukos, *J. Periodontal Res.* **2009**, 44, 751–769.
- [36] J. L. Wardlaw, T. J. Sullivan, C. N. Lux, F. W. Austin, *The Veterinary Journal* **2012**, 192, 374–377.
- [37] M. Wainwright, *J. Antimicrob. Chemotherapy* **2004**, 48, 2173–2178.
- [38] R. K. Pandey, unpublished results.
- [39] J. F. Lovell, J. Chen, M. T. Jarvi, W. G. Cao, A. D. Allen, Y. Liu, T. T. Tidwell, B. C. Wilson, G. Zheng, *J. Phys. Chem. B* **2009**, 113, 3203–3211.
- [40] S. K. Pandey, A. L. Gryshuk, M. Sajjad, X. Zheng, Y. Chen, M. M. Abouzeid, J. Morgan, H. A. Nabi, A. Oseroff, R. K. Pandey, *J. Med. Chem.* **2005**, 48, 6286–6295.
- [41] C. Alonso, R. W. Boyle, Chapter 17 in *Handbook of Porphyrin Science* (Eds. K. M. Kadish, K. M. Smith, R. Guilard), World Scientific, New Jersey, **2010**.
- [42] L. N. Goswami, M. Ethirajan, M. P. Dobhal, M. Zheng, J. R. Missert, M. Shibata, K. M. Kadish, R. K. Pandey, *J. Org. Chem.* **2009**, 74, 568–579.
- [43] P. Salice, J. Arnbjerg, B. W. Pedersen, R. Toftgaard, L. Beverina, G. A. Oagani, P. R. Ogiby, *J. Phys. Chem. A* **2010**, 114, 2518–2525.
- [44] O. S. Finikova, P. Chen, Z. Ou, K. M. Kadish, S. A. Vinogradov, *J. Photochem. Photobiol. A* **2008**, 198, 75–84.
- [45] D. Rehm, A. Weller, *Isr. J. Chem.* **1970**, 8, 259–271.
- [46] S. K. Pandey, X. Zheng, J. Morgan, J. R. Missert, T. H. Liu, M. Shibata, D. A. Bellnier, A. R. Oseroff, B. W. Henderson, T. J. Dougherty, R. K. Pandey, *Mol. Pharm.* **2007**, 4, 448–464.
- [47] X. Q. Lin, K. M. Kadish, *Anal. Chem.* **1985**, 57, 1498–1501.

Received: October 29, 2012

Revised: January 22, 2013

Published online: March 22, 2013